Applied Soft Computing Journal 76 (2019) 744–762

Contents lists available at ScienceDirect

Applied Soft Computing Journal

journal homepage: www.elsevier.com/locate/asoc

Multichannel image contrast enhancement based on linguistic rule-based intensificators

Hoang Huy Ngo [b,c], Cat Ho Nguyen [a,*], Van Quyen Nguyen [d]

[a] *Institute of Theoretical and Applied Research at Hanoi, Duy Tan University, Danang, Viet Nam*
[b] *Institute of Information Technology, VAST, Hanoi, Viet Nam*
[c] *Electric Power University of the Vietnam Ministry of Industry and Trade, Hanoi, Viet Nam*
[d] *Department of Postgraduate Management, Haiphong University, Haiphong, Viet Nam*

HIGHLIGHTS

- Develop an RGB-image contrast intensificator (*CI*) immediately handing expert linguistic rule bases, *Hint*.
- Define pixelwise-defined operators influencing on the *CI*-performance to control the balance between global and local image features.
- Establish a HA-formalism to soundly converse such linguistic rules to S-function to construct a desired *CI*.
- Apply for the first time standard FCM, $F\mathfrak{C}_{fz}$, to entire RGB-images to reveal regional image features.
- The proposed method - an integration of *Hint* using a new surrounding luminance operator and $F\mathfrak{C}_{fz}$ - is run on 27 RGB-images to show its effectiveness.

GRAPHICAL ABSTRACT

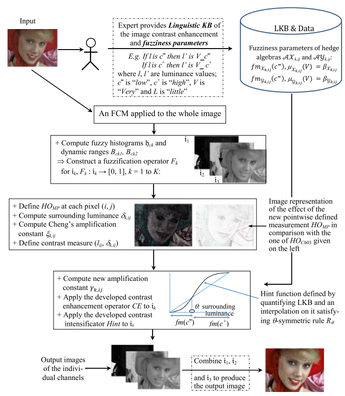

ARTICLE INFO

Article history:
Received 29 March 2017
Received in revised form 6 November 2018
Accepted 23 December 2018
Available online 7 January 2019

Keywords:
Image contrast enhancement
Contrast measurement
Hedge algebra
Linguistic rule-based knowledge
Interpolation inference method

ABSTRACT

This study follows the direct approach to image contrast enhancement, which changes the image contrast at each its pixel and is more effective than the indirect approach that deals with image histograms. However, there are only few studies following the direct approach because, by its nature, it is very complex. Additionally, it is difficult to develop an effective method since it is required to keep a balance in maintaining local and global image features while changing the contrast at each individual pixel. Moreover, raw images obtained from many sources randomly influenced by many external factors can be considered as fuzzy uncertain data. In this context, we propose a novel method to apply and immediately handle expert fuzzy linguistic knowledge of image contrast enhancement to simulate human capability in using natural language. The formalism developed in the study is based on hedge algebras considered as a theory, which can immediately handle linguistic words of variables. This allows the proposed method to produce an image contrast intensificator from a given expert linguistic rule base. A technique to preserve global as well as local image features is proposed based on a fuzzy clustering method, which is applied for the first time in this field to reveal region image features of raw images. The projections of the obtained clusters on each channel are suitably aggregated to produce a new channel image considered as input of the pixelwise defined operators proposed in this study. Many experiments are performed to demonstrate the effect of the proposed method versus the counterparts considered.

* Corresponding author.
E-mail address: nguyencatho@duytan.edu.vn (C.H. Nguyen).

https://doi.org/10.1016/j.asoc.2018.12.034

1. Introduction

Images provide necessary information in various practical fields; however, raw images usually are of low quality, because when capturing them, they are usually affected by many random factors, for instance, the equipment to capture the images and lighted condition or real-life condition. Therefore, in general, they suffer from poor contrast and noise, even occlusion, and hence, they hide image details that may involve meaningful and useful information. To enhance the image quality, image contrast enhancement (ICE) plays an important role in medical images [1–4], biomedical images [5–7], satellite images [8–14], microscopic images [15–17], human/machine vision [18,19], and even real-life photographs. Because, in practice, many factors affecting the quality of captured images are random or uncertain in nature, they make images and their details fuzzy. Thus, it is required to develop a soft formalism to handle their fuzziness. This leads to apply the fuzzy set theory to the field of image processing and analysis [20–35].

ICE techniques attract much attention in the image processing community to improve the image interpretability or visualisation or to bring out useful information hidden in image details. Many contrast enhancement algorithms (most of them rely on the indirect approach that changes the histogram without defining any specific contrast measure), can be found in the literature, e.g. those based on changing the contrast measurement [36,37], changing the contrast using square, log, or exponential functions [38], using the fuzzy entropy principle or, as aforementioned, using the fuzzy set theory. Many other techniques for image enhancement are exploited, e.g. global histogram equalisation [39], logarithmic transform histogram shifting and histogram-based image enhancement [40], dynamic histogram equalisation technique [41], multi-histogram normalisation method [42], and discrete cosine transform [43]. However, only few studies follow the direct approach that modify the image contrast at each pixel of the image, e.g. [21,22,38,44,45]. In [38,44], it is proved that the direct method offers techniques that can produce more effective results.

The uncertainty-based approaches exploit relatively different philosophy and formalisms of the fuzzy set theory [22,32,33]. In these approaches, images are represented as two-dimension fuzzy sets to which fuzzy set-based methods are applied to utilise fuzzy set formalism to handle uncertainty, including the use of type I fuzzy sets [21,22,27,32,33] or type II fuzzy sets, and fuzzy inference methods, e.g. [10]. These methods are very flexible and are especially capable of simulating human ability in handling linguistic knowledge bases (LKBs), particularly in reasoning based on fuzzy set representations of LKBs. Most methods of the aforementioned studies on the indirect approach are executed based on a fuzzy formalism, but not many of them developed fuzzy inference techniques using fuzzy rule bases, e.g. [28,35].

As mentioned above, two studies by Cheng and Xu [21,22] follow the direct approach to modify the contrast at each image pixel by applying a contrast measure pixelwise defined based on the difference between the luminance at each image point and one of its prespecified surrounding region. These two studies apply a fuzzy set-based formalism in which the fuzziness of the contrast at each image point is represented by an S function with parameters defined by utilising certain local image features. Based on this, they propose new intensification contrast enhancements to modify the S-function shapes, which are shown to be more effective and efficient than the counterpart methods based on the indirect approach. Note that as commented by Hanmandlu and Jha [46], the application of a colour image enhancement on the RGB colour model using a histogram equalisation technique is inappropriate for the human visual system because it fails when applied to the three components (R, G, B) of a degraded colour image by losing its original colour composition.

Although the motivation for applying fuzzy rule bases, whose fuzzy sets are assigned to linguistic labels, and approximate reasoning methods is to simulate human capabilities in immediately manipulating their own linguistic words, in nature, they have no prescribed formalism to deal immediately with words of variables. Hedge algebras (HAs) are mathematical models of word domains of variables developed based on inherent word semantics. They provide sound formalisms to immediately handle words [47,48] and their computational (compt.-) semantics, in which the inherent qualitative semantics of words does determine their compt.-semantics [49–52]. It is shown that they can be applied to solve many practical problems effectively in distinct areas [49–51,53–59].

Because human beings are familiar with the use of their own words to render their experience and knowledge to solve practical problems, the study aims to propose a novel method of utilising this human expertise in using their own linguistic knowledge to change the image contrast. The method has three main distinguished features:

- Ability to utilise the distinctive capability of a human expert in representing his/her experience to enhance the image contrast in terms of his/her own linguistic rules, called *linguistic model*, in which appear words of the luminance variable such *very dark* or *slightly darker*, whose hedges play a specific role in expressing his/her experience. It is interesting that linguistic models of this problem always describe increasingly monotonic linguistic functions that can be utilised to produce S functions to enhance the image contrast.
- Applying the semantically quantifying mappings of word domains of the luminance variables to produce a numeric S function at each image pixel defined in a two-dimensional luminance space from the expert linguistic model, while preserving its monotonicity. This S function can be easily modified by changing only few fuzziness parameters of the luminance variable. Some characteristics of the input images are also utilised to ensure suitability of the desired S function.
- Two main techniques dealing with multichannels of images are developed to achieve a suitable balance between global image features and local ones. The first one is to deal with the image operators proposed to act on multichannel images but are pixelwise defined in each channel. The other is to apply for the first time a fuzzy clustering method (FCM) in this field to make use of the global image features revealed by the FCM. It is first applied to cluster the whole raw multichannel image, and then, the projections of the obtained clusters on each channel are aggregated by an appropriate linear transformation to form an input image of the above-mentioned proposed operators.

This paper is organised as follows: In Section 2, some necessary knowledge of the direct approach to ICE and HAs to examine the study are presented. Section 3 is devoted to establishing a formalised foundation based on the theory of HAs for developing the image contrast intensificator (*CI*). The proposed method of image contrast intensification with a reasoning method developed based on an HA formalism is presented in Section 4. A comparative study of the proposed method with its counterparts based on many experiments is given in Section 5. Conclusions are provided in Section 6.

2. Background

2.1. Necessary knowledge of HAs for modelling the semantics of linguistic rules

Because human beings are familiar with their own linguistic words to render their experience or cognition or doing reasoning in

Table 1
Relative sign of a hedge in a row with respect to a hedge in a column.

sign (h, k)	*E*	*V*	*R*	*L*
E	+	+	−	+
V	+	+	−	+
R	−	−	+	−
L	−	−	+	−

terms of words and if-then rules to solve practical problems, in this study, we will show that HAs and their quantification theory enable us to make use of these human capabilities in the field of ICE based on an appropriate formalism that is capable of dealing immediately with expert linguistic rules. Note that there is no formal basis in the fuzzy set framework to immediately handle human words of variables and their inherent semantics, and in addition, the word domains are still not formalised.

HAs, introduced in [47,48] establish an algebraic approach to formalise word domains of variables based on the inherent order-based semantics of their words. This viewpoint is also supported by observation that the comparability between words in a word domain is a consequence of the demand for decision-making activities in human daily life, in which pairwise comparisons of decision alternatives in terms of linguistics are crucial. Consequently, there are comparability elements in human languages. For example, for every hedge h, say *very* (V) of the luminance variable $\mathcal{X}$, the words *very bright* and *bright*, for example, are always comparable. Therefore, as the luminance space is linear, the word domain Dom($\mathcal{X}$) may be assumed to be a linearly ordered set and can be formalised as an abstract algebra, denoted by $\mathcal{AX} = (\text{Dom}(\mathcal{X}), G, C, H, \leq)$, where $G = \{dark, bright\}$ is the set of atomic (primary) terms considered as the generators of $\mathcal{AX}$; C is the set of constants $C = \{\mathbf{0}, W, \mathbf{1}\}$, which are, respectively, the least, neutral, and greatest words of Dom($\mathcal{X}$); $H = H^- \cup H^+$ is the set of hedges of $\mathcal{X}$, regarded as unary operations, where H^- (or H^+) is the set of negative (or positive) hedges, e.g. $H^- = \{R\}$ and $H^+ = \{V\}$; and $\leq$ is the semantic order relation (SOR). Syntactically, Dom($\mathcal{X}$) is the set of all strings in the form $h_n \ldots h_1c$, $c \in G$ and h_i's $\in H$, of $\mathcal{X}$.

2.1.1. Description of HA formalisation

In the HA approach to word semantics, the word domain of every $\mathcal{X}$ is formalised as an order-based structure, $\mathcal{AX} = (\text{Dom}(\mathcal{X}), G, C, H, \leq)$, whose axioms are certain of the following discovered properties of words and hedges of $\mathcal{X}$ formulated in terms of *SOR* $\leq$ [47,60,61]:

- Words of $\mathcal{X}$ have its own 'algebraic' signs computed as follows. For atom words, conventionally, we have

(i) $sign(c^-) = -1$ and $sign(c^+) = +1$;

(ii) For any hedge h, $sign(h) = +1$ iff $h \in H^+$ or $hc^+ \geq c^+$ and $sign(h) = -1$ iff $h \in H^-$ or $hc^+ \leq c^+$;

(iii) The relative sign of h with respect to k, denoted by $sign(h, k)$, is computed by $sign(h, k) = -1$ iff $(\exists c \in G)(kc \leq c \Rightarrow kc \leq hkc)$ and $sign(h, k) = +1$ iff $(\exists c \in G)(kc \leq c \Rightarrow hkc \leq kc)$. See Table 1 for illustration.

(iv) The sign of $x = h_n \ldots h_1c$ is defined by $sign(x) = sign(h_n, h_{n-1}) \ldots sign(h_1)sign(c) \in \{-1, +1\}$. Then, we have $sign(hx) = -1$ leading to $hx \leq x$, and $sign(hx) = +1$ leading to $x \leq hx$. For example, $sign(VR\_dark) = sign(V,R)sign(R) \times sign(dark) = -1$, which implies that $VR\_dark \leq R\_dark$.

- For every $h \in H$ and every word $x \in \text{Dom}(\mathcal{X})$, we have either $x \leq hx$ or $x \geq hx$, and by the functionality of hedges, the word hx inherits the semantics of its parent x, called *hedge inheritance*, which can be formalised as follows: $hx \leq kx \Rightarrow H(hx) \leq H(kx)$, $\forall h, k$, where $H(z) = \{\sigma z : \sigma = h_n \ldots h_1 \in H^*, \varnothing \in H^*\}$, which states that any strings of hedges σ and σ' applying to hx and kx cannot change the direction of $hx \leq kx$, i.e. we still have $\sigma hx \leq \sigma' kx$. Thus, $H(x)$ can be considered as a *fuzziness model* of x. The set $\{H(x): x \in \text{Dom}(\mathcal{X})\}$ can be arranged as a multilevel structure given in Part 1, Fig. 1, in which the $H(x)$'s on the same level, whose x's have the same length, are linearly ordered.

2.1.2. Key compt.-semantic aspects of the words of variable domains (see [61,62])

The quantification of any $\mathcal{AX}$ can be developed under the principle that the inherent qualitative semantics of the words of $\mathcal{X}$ should formally determine their respective compt.-semantics. Clearly, the word semantics is a complex and inexact concept, while the semantics of compt.-quantities, such as numeric values and intervals, are much simpler ones. Thus, to adequately and accurately represent the word semantics in terms of compt.-objects, it is required to use different types of compt.-objects, each of which expresses an aspect of the word semantics as follows:

- *Numeric semantics of words*. A mapping $f : \boldsymbol{X} \to [0, 1]$, where [0, 1] is the normalised universe of $\mathcal{X}$, is said to be a numeric semantics interpretation if it is an *order isomorphism*, whose image $f(\boldsymbol{X})$ is dense in [0, 1]. It is called a *semantically quantifying mapping* (SQM) and, by its nature, its values can be interpreted as the numeric semantics of the words.

- *Interval semantics and fuzziness measure of the words of* $\mathcal{X}$. An SQM f can map each $H(x)$ to a subinterval of [0, 1] which is the closure of the set $f(H(x))$ and denoted by $\Im(x) = [f(H(x))]$, as depicted in Fig. 1, and called the fuzziness interval or an interval semantics of x. Its length is called fuzziness measure of x and denoted by $fm(x)$. Therefore, f transforms the structure of $H(x)$'s to a compt.-structure of the interval semantics of words, as shown in Part 2 of Fig. 1. It offers many useful compt.-semantic properties of words. For instance, putting $\alpha = \sum_{h \in H^-} \frac{fm(hx)}{fm(x)}$ and $\beta = \sum_{h \in H^+} \frac{fm(hx)}{fm(x)}$, from the structure exposed in Fig. 1, it follows that

$$\sum_{h \in H} fm\,(hx) = fm(x) \text{ and } \sum_{h \in H} \mu(h) = \alpha + \beta = 1 \quad (1)$$

where we adopt the hypothesis that for all j, the fraction $\frac{fm(h_jx)}{fm(x)}$ is independent of a particular x. It is denoted by $\mu(h_j)$ and called the effect or the fuzziness measure of h_j. Thus, we have

$$fm(c^-) + fm(c^+) = 1 \quad (2)$$

$$fm(hx) = \mu(h)fm(x), \text{ for all } x \text{ and } h \quad (3)$$

In the HA approach, the conditions (1) to (3) can be considered as the axioms to define fm, and therefore, it is called the fuzziness measure of the whole variable $\mathcal{X}$. This shows that the interval semantics and the SQM values of all words of $\mathcal{X}$ can be completely computed when the quantities $fm(c^-)$, $fm(c^+)$, and $\mu(h_j)$'s, called fuzziness parameters of $\mathcal{X}$, are known.

Example 1. Assume that the syntactic semantics of current intensity variable $\mathcal{I}$, whose universe is [0, 10] in amperes, is defined by the sets $G = \{s\ (small), l\ (large)\}$, $H^- = \{L, R\}$, and $H^+ = \{V, E\}$, whose relative signs are given in Table 1. The compt.-semantics of its words can be computed by providing the numeric values of the independent fuzziness parameters as follows: $fm(s) = 0.6$, $\mu(L) = 0.15$, $\mu(R) = 0.3$, and $\mu(V) = 0.35$. Then, the aforementioned quantitative semantics of any word of the variable $\mathcal{I}$ can be easily computed. For example, given a word $x = RVs$,

∘ The fuzziness measure $fm(RVs)$ is calculated as follows:

$$fm(x) = \mu(R) \cdot \mu(V) \cdot fm(s) = 0.3 \times 0.35 \times 0.6 = 0.063$$

∘ Calculate its fuzziness interval, $\Im(RVs)$. Because $|\Im(RVs)|$ = 0.063, it is sufficient to calculate the left-point($\Im(RVs)$). From Fig. 2, we infer that $\Im(s) = \Im(Es) \cup \Im(Vs) \cup \Im(Rs) \cup \Im(Ls)$ and $\Im(Vs)$ =

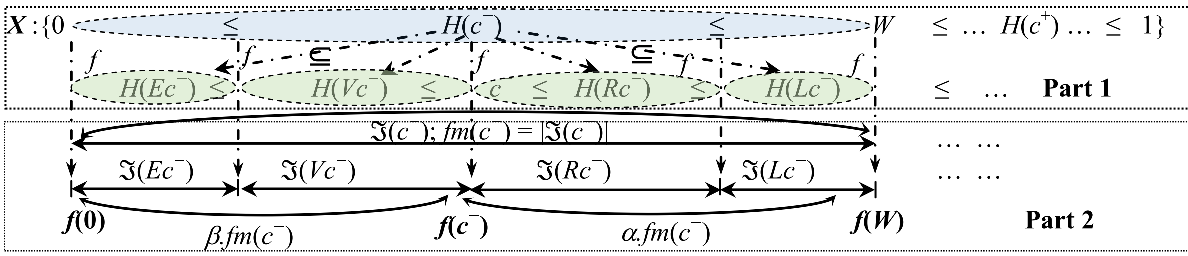

Fig. 1. Multilevel semantic structure of Dom($\mathcal{X}$) and corresponding multilevel structure of fuzziness intervals of its words.

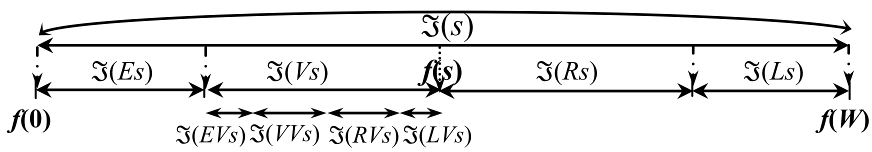

Fig. 2. A piece substructure of fuzziness intervals of some words included in $\Im(s)$.

$\Im(EVs) \cup \Im(VVs) \cup \Im(RVs) \cup \Im(LVs)$, whose subintervals are ordered from left to right. Thus, left-point($\Im(RVs)$) = left-point ($\Im(Vs)$) + $|\Im(EVs)|$ + $|\Im(VVs)|$ = $|\Im(Es)|$ + $|\Im(EVs)|$ + $|\Im(VVs)|$ = $(\mu(E) + \mu(E)\mu(V) + \mu(V)^2)fm(s) = (0.2 + 0.2 \times 0.35 + (0.35)^2) \times 0.6 = 0.2355$. Thus, on the universe [0, 10] in amperes, $\Im(RVs)$ = [2.355, 2.355 + 10 × $|\Im(RVs)|$] = [2.355, 2.985].

- *Methods of computing numeric semantics of words*. Assume that $\mathcal{AX}$ and its fuzziness parameter values are given. There are two ways of calculating the numeric semantics or f values:

(A) Calculate the SQM values of words immediately based on the fuzziness interval structure given in Fig. 1. For a given word x, it is observed from Fig. 1 or 2 that $f(x)$ is just the common value of $\Im(h_{-1}x)$ and $\Im(h_{+1}x)$ of $\Im(x)$, where $h_{-1} = R$, $h_{+1} = V$, noting that $\Im(h_{+1}x)$ is on the right of $f(x)$, if $sign(h_{+1}x) = +1$, or on the left of $f(x)$, if $sign(h_{+1}x) = -1$. Thus, $f(x)$ is calculated as follows:

(i) Calculate and locate the fuzziness intervals $\Im(h_{-1}x)$ and $\Im(h_{+1}x)$ in [0, 1];

(ii) Then, $f(x) =$

$$\begin{cases} \text{left\_point}\left(\Im(x)\right) + \beta\,|\Im(x)| & \text{if } sign\,(h_{+1}x) = -1 \\ \text{left\_point}\left(\Im(x)\right) + \alpha\,|\Im(x)| & \text{if } sign\,(h_{+1}x) = +1 \end{cases} \tag{4}$$

(B) Recursive formula to compute $f(x)$. As $f(x)$ divides $\Im(x)$ in the proportion $\beta : \alpha$ (or, $\alpha : \beta$) if $sign(h_p x) = -1$ (or, $sign(h_p x) = +1$), the recursive formula is established as follows [62]:

(SQM1) $f(\boldsymbol{W}) = fm(c^-), f(c^-) = \beta fm(c^-), f(c^+) = f(\boldsymbol{W}) + \alpha fm(c^+)$;

(SQM2) $f\left(h_j x\right)$

$$= f\,(x) + sign(h_j x)\left\{\sum_{i=sign(j)}^{j} fm(h_i x) - \vartheta\left(h_j x\right) fm(h_j x)\right\} \tag{5}$$

where $\vartheta\left(h_j x\right) = 0.5\left[1 + sign\left(h_j x\right) sign\left(h_p h_j x\right)(\beta - \alpha)\right] \in \{\alpha, \beta\}$, for $\forall j \neq 0$ and $-q \leq j \leq p$.

It is worth emphasising that although the numeric semantics of the words are crisp values, they are defined in the context of the fuzziness of words by giving the fuzziness parameters of $\mathcal{X}$. That is, they still convey the fuzziness of words of $\mathcal{X}$. Moreover, it is important that these quantitative quantities of $\mathcal{X}$ are defined in the context of the entire $\mathcal{X}$.

Example 2. This example aims to illustrate how one can compute the compt.-semantics of a variable, say the luminance variable $\mathcal{L}$ of an image.

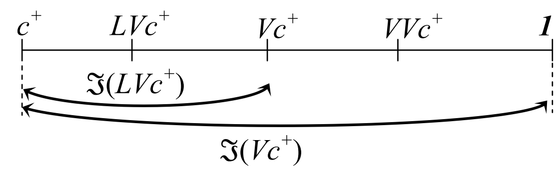

Fig. 3. Position of $\Im(LVc^+)$.

Task 1. Determine the syntax semantics of $\mathcal{L}$ to produce its word domain appropriate to a given application. Because every word of the variable is a string generated from an atom $c \in \{c^-, c^+\}$ by hedges in the set H of $\mathcal{L}$, its semantics depends strongly on how many and which hedges of $\mathcal{L}$ the expert expects to be appropriate to his/her domain application. For simplicity, assume that they are two hedges *Very* (V) and *Little* (L). Then, Dom($\mathcal{L}$) is syntactically determined.

Task 2. Determine the compt.-semantics of the words of $\mathcal{L}$. To calculate the above quantitative characteristics of all words of $\mathcal{L}$ instead of designing a fuzzy set of each individual word, the expert needs only to assign intended numeric values to merely few independent fuzziness parameters of $\mathcal{L}$. Applying (1) to (5), all the compt.-semantics of any words of $\mathcal{L}$ can always be calculated.

For example, compute the compt.-semantics of $x = LVbright$ with $fm(c^-) = 0.45$ and $\mu(V) = 0.55$ using the method described in point (A). Clearly, $\beta = \mu(V) = 0.55$, $\alpha = \mu(L) = 1 - \mu(V) = 0.45$. Then, we locate the fuzziness interval $\Im(x)$ as follows: By (3), we have, $|\Im(x)| = fm(LVc^+) = \mu(L){\cdot}\mu(V){\cdot}fm(c^+) = (1 - 0.55) \times 0.55 \times (1 - 0.45) = 0.136125$. Referring to Fig. 3, *left-point*($\Im(LVc^+)$) = *left-point*($\Im(Vc^+)$) = $1 - |\Im(Vc^+)| = 1 - \mu(V){\cdot}fm(c^+) = 1 - 0.3025 = 0.6975$. To compute $f(LVc^+)$, from Table 1, we have $sign(VLVc^+) = sign(V, L){\cdot}sign(L, V){\cdot}sign(V){\cdot}sign(c^+) = (+1)(-1)(+1)(+1) = -1$. Therefore, by (4), $f(LVc^+) = 0.6975 + \beta|\Im(LVc^+)| = 0.6975 + 0.55 \times 0.136125 \approx 0.772369$.

Now, the actual luminance of x is $0.772369 \times 255 \approx 196.95 \in [0, 255]$.

2.2. Semantics of LKBs and their ability to describe ICE

To simulate human capabilities in handling words immediately, the proposed method permits an expert to express his/her desired ICE of a given raw image in terms of linguistic rules based on his/her experience that form an LKB. We will show that although an LKB used in the experiment section is still very simple, it can already show its considerable effect. Assume that the LKB $\mathcal{LB}$ given by the expert to represent a relation between the luminance variable $\mathcal{X}$ of an input image $\mathbb{i}$ with domain $[L_{\mathbb{i},\min}, L_{\mathbb{i},\max}]$ and the luminance variable $\mathcal{Y}$ of his/her desired output $\mathbb{i}'$ with domain $[L_{\mathbb{i}',\min}, L_{\mathbb{i}',\max}]$ consists of n rules:

$$(r_k) \text{ IF } \mathcal{X} \text{ is } x_k \text{ THEN } \mathcal{Y} \text{ is } y_k, \text{ for } k = 1, \ldots, n \tag{6}$$

where x_k and y_k are words of $\mathcal{X}$ and $\mathcal{Y}$, respectively. Similar to that in fuzzy approaches, in the HA approach, every reasoning method working on $\mathcal{LB}$ can produce a curve f: $[L_{\mathbb{i},\min}, L_{\mathbb{i},\max}] \to [L_{\mathbb{i}',\min}, L_{\mathbb{i}',\max}]$. Because $\mathcal{LB}$ given by an expert describes linguistically a change in image luminance to enhance the image contrast of $\mathbb{i}$, $f(\mathbb{i})$ represents an output image $\mathbb{i}'$ that he/she expects, when applying a suitable reasoning method. In this study, the reasoning method is constructed as follows:

- Construct appropriate HAs $\mathcal{AX}$ and $\mathcal{AY}$ of variables $\mathcal{X}$ and $\mathcal{Y}$ by selecting their suitable hedges (maybe one positive hedge and one negative hedge, for simplicity) and determine their independent fuzziness parameter values based on calculating certain local physical features of $\mathbb{i}$.
- Compute the SQM values of the words appearing in $\mathcal{LB}$ using the determined fuzziness parameter values of $\mathcal{X}$ and $\mathcal{Y}$. Then, the compt.-semantics of $\mathcal{LB}$ is represented by a grid of n points in the Cartesian space $[0, 1]^2$, which describes a curve f running through these grid points, where $[L_{\mathbb{i},min}, L_{\mathbb{i},\max}]$ and $[L_{\mathbb{i}',\min}, L_{\mathbb{i}',\max}]$ are both normalised into [0, 1].
- Construct an interpolation method to calculate approximately the curve f so that it preserves the order-based semantics of $\mathcal{LB}$. This requirement is essential because the nature of ICE implies that $\mathcal{LB}$ is always increasingly monotonic.

We interpret the reasoning method applied in the study to be proper because it is developed based on a sound approach to the word semantics, as previously discussed, and the numeric interpolation method is constructed to preserve the monotonicity of $\mathcal{LB}$.

3. HA-based formal basis for developing image contrast intensification methods

In this section, we propose a formal basis for developing methods of enhancing the image quality by intensifying the image contrast at every image pixel using expert experiences expressed in terms of his/her LKB. In the HA approach, every LKB consisting of n linguistic rules with m input variables and one output variable, whose word domains are modelled by their respective HAs, can be viewed as representing a linguistic function in the Cartesian product of (m + 1) HAs. Using SQMs presented in Section 2, one can transform this LKB representing expert domain experience into a grid of n points that approximately represents a function in $[0, 1]^{m+1}$. This formalism suggests that every method of image contrast intensification can be considered as an operator CI, which is pixelwise defined when acting on an image $\mathbb{i}$. As such, a CI is practically complex, and it should be analysed as a combination of specific component operators in order to develop effective CIs easily. Thus, we discuss first the component operators of a general CI and then we construct a CI which is able to deal with expert LKBs based on an HA-based formalism called HA-based CI and denoted by *Hint*.

3.1. Analysis of image CI based on contrast enhancement

As mentioned previously, we will deal with images of multichannels, which are closely related to each other. A contrast enhancement method of the direct approach applied to an image can be considered as an ICE operator $\mathcal{E}$ acting on an κ-channel image $\mathbb{i}$ represented as an array $\{p_{i,j} : (i,j) \in M \times N\}$, where the pixel p_{ij} is represented as a mapping vector $\mathfrak{i}(p_{ij}) = (\mathfrak{i}_1(p_{ij}), \ldots, \mathfrak{i}_\kappa(p_{ij})) = l_{ij}$, where $\mathfrak{i}_k : \{p_{i,j} : (i,j) \in M \times N\} \to [L_{k,min}, L_{k,max}]$, i.e. $l_{k,ij} = \mathfrak{i}_\kappa(p_{ij}) \in [L_{k,min}, L_{k,max}]$, for $k = 1$ to κ, are mappings. For simplicity, hereafter, it should be noted that every multichannel image $\mathbb{i}$ is identical with this vector mapping $\mathfrak{i}$.

We propose a new method of ICE consisting of few steps performed by certain image operators having specific properties, some of which deal with images as a whole and the remaining ones deal with individual channels. In this way, we may assess the performance of each operator to improve the image quality. First, we consider an arbitrary kth channel of an image $\mathbb{i}$, denoted also by $\mathbb{i}$, for simplicity, when no confusion occurs. The problem of the ICE of $\mathbb{i}$ (the kth channel) is to find an ICE operator $\mathcal{E}$ that can transform the image $\mathbb{i}$ into $\mathcal{E}(\mathbb{i})$ of as high quality as possible with respect to certain criteria. For convenience, every ICE operator based on a fuzzy approach applying to each image channel is decomposed into the following pixelwise-defined operators:

- *Fuzzificator F*. For a given increasingly monotonic function f : $[L_{min}, L_{max}] \to \mathbb{I}_L = [0, 1]$, whose inverse function is f^{-1}, the fuzzificator defined by f is a mapping $F_f : \mathbb{i} = \{l_{i,j} : (i,j) \in M \times N\} \to F_f(\mathbb{i}) = \{f(l_{i,j}) : (i,j) \in M \times N\}$, for every image $\mathbb{i}$. Therefore, given an $\mathbb{i}$, $F_f(\mathbb{i})$ is a fuzzy set representing the fuzziness of $\mathbb{i}$ restricted to the channel in question defined by means of the given f. Thus, F_f is a factor that can actually change the luminance to enhance the image contrast.

- *Surrounding luminance operator* $\mathcal{S}$. This operator determines a surrounding luminance in a given window W of every pixel of $F_f(\mathbb{i})$, $\mathcal{S} : F_f(\mathbb{i}) \to \mathcal{S}(F_f(\mathbb{i})) = \{\mathcal{S}(f(l_{i,j}), W_{ij}) \in \mathbb{I}_L = [0,1] : (i,j) \in M \times N\}$, i.e. for every pixel p_{ij}, $\mathcal{S}$ defines a surrounding luminance b_{ij} of $f(l_{i,j})$. For the case of f being a linear transformation to normalise the reference domain into [0, 1], $\mathcal{S}$ is simply written as $\mathcal{S}$: $\mathbb{i} \to \mathcal{S}(\mathbb{i}) = \{\mathcal{S}(l_{i,j}, W_{ij}) \in \mathbb{I}_L : (i,j) \in M \times N\}$. For illustration, the new concept of homogeneity HO_{ij} defined and calculated in [21] using certain local features of $\mathbb{i}$ can be considered as $\mathcal{S}$.

- *Contrast measure operator* $\mathcal{C}_{\mathbb{c},b}$. This operator aims to compute a contrast measure at a pixel p of $F_f(\mathbb{i})$ with respect to a given surrounding luminance b of p. Given a (contrast measurement) function $\mathbb{c}(b, l) \in \mathbb{I}_{\mathbb{c}} = [0, 1]$, b, $l \in \mathbb{I}_L = [0, 1]$, satisfying the condition that for any $b \in \mathbb{I}_L$, $\mathbb{c}(b, b) = 0$ and the function $\mathbb{c}(b, .)$ is continuous and piecewise strictly monotonic in each interval of [0, b] and [b, 1]. To avoid possible confusion, the notation $\mathbb{I}_{\mathbb{c}}$ is used to highlight that although its values are also in the (normalised) luminance domain [0, 1], they indicate the contrast measure of the image pixels but not the luminance values. There are some definitions of the contrast measure of image pixels in the literature. In this study, we apply the contrast measure used in [21]:

$$\mathbb{c}(b, l) = \frac{|l - b|}{|l + b|} \in \mathbb{I}_{\mathbb{c}} = [0, 1] \tag{7}$$

Set $\mathbb{c}(\mathcal{S}(\mathbb{i})) = \{\mathbb{c}(b_{ij}, f(l_{i,j})) : (i,j) \in M \times N\}$, where $b_{ij} = \mathcal{S}(l_{ij}, W_{ij})$.

Then, given $\mathbb{c}$, the contrast measure operator is defined pixelwise as follows:

$\mathcal{C}_{\mathbb{c}} : \mathbb{i} \to \{\mathbb{c}(b_{ij}, f(l_{i,j})) : (i,j) \in M \times N\}$, i.e. $\mathcal{C}_{\mathbb{c}}(\mathbb{i}) = \mathbb{c}(\mathcal{S}(\mathbb{i}))$

For simplicity, fix a pixel $p_{ij} = p$ and put $b = b_{ij}$ and $l = f(l_{ij})$, by (7); we have $\mathcal{C}_{\mathbb{c},b}(l) = \mathbb{c}(b, l) \in \mathbb{I}_{\mathbb{c}}$, which defines a function $\mathcal{C}_{\mathbb{c},b}(l)$ of the luminance at p. Because $\mathcal{C}_{\mathbb{c},b}$ is invertible in each interval of [0, b] and [b, 1], we may determine the inverse $\mathcal{C}^{-1}_{\mathbb{c},b}$ of $\mathcal{C}_{\mathbb{c},b}$, where $\mathcal{C}^{-1}_{\mathbb{c},b}$: $\mathbb{I}_L = [0, 1] \to \mathbb{I}_{\mathbb{c}}$. Thus, $\mathcal{C}_{\mathbb{c},b}(l)$ is the contrast measurement of the image at pixel p and, for a given contrast degree $s \in \mathbb{I}_{\mathbb{c}}$ at a pixel p, $\mathcal{C}^{-1}_{\mathbb{c},b}$ $(s)$is the luminance at p having the contrast degree s.

- *Contrast intensificator* $CI_{\mathbb{c}}$ *and contrast enhancement operator CE with a given contrast measurement* $\mathbb{c}$. The operator $CI_{\mathbb{c}}$, which intensifies the contrast of $\mathbb{i}$, is also pixelwise defined using the operator $\mathcal{S}$ to compute the surrounding luminance of each pixel. Let CI: $\mathbb{I}_{\mathcal{S}} \times \mathbb{I}_L \times \mathbb{I}_{\mathbb{c}} \to \mathbb{I}_L$ be any function, where, similar to $\mathbb{I}_{\mathbb{c}}$, $\mathbb{I}_{\mathcal{S}}$ is used instead of $\mathbb{I}_L$ to indicate its values to be the surrounding luminance values of its pixels. For any $b \in \mathbb{I}_{\mathcal{S}} = [0, 1]$ and $c \in \mathbb{I}_{\mathbb{c}}$ =

[0, 1], the function $CI_{b,c}$: $\mathbb{I}_L \to \mathbb{I}_L$ defined by $CI_{b,c}(l) = CI(l, b, c)$ is said to be a contrast intensification function with respect to b, if it satisfies the following condition for every $l \in [0, 1]$:

$$\begin{cases} CI_{b,c}(l) = b, & \text{for } l = b \\ CI_{b,c}(l) \le l, & \text{for } 0 \le l < b \\ CI_{b,c}(l) \ge l, & \text{for } b < l \le 1 \end{cases} \tag{8}$$

In the direct approach, because CI is pixelwise defined, the notation $CI_{b,c}(l)$ is useful to change the luminance l at every pixel based on the surrounding value b and the contrast value c computed using the given $\mathbb{c}$. The function of $CI_{b,c}$ is to change the luminance l at a pixel into a luminance $l' = CI_{b,c}(l)$ so that the new contrast degree expected by an expert can be expressed by a contrast enhancement operator, denoted by CE, which is defined as follows:

∘ *Contrast enhancement operator CE*. The operator $CE : \mathbb{I}_c \to \mathbb{I}_c$, which enhances the contrast measurement of an image pixel, is characterised by the following condition:

$$CE(c) \ge c, \text{ for all } c \in \mathbb{I}_{\mathbb{c}} \tag{9}$$

Thus, while CI is the operator that changes the luminance at each pixel of an image in such a way that its contrast is enhanced, the functionality of CE is to change only the contrast of every image pixel. The relation between $CI_{\mathbb{c}}$ and CE is expressed by the following constraint:

$$c(b, CI_{b,c}(l)) = CE(CI_{b,c}(l)) \ge c \tag{10}$$

Then, the operator $CI_{b,c}$, which is defined based on the contrast measure operator $\mathcal{C}_{\mathbb{c},b}$ and a contrast enhancement operator CE, can be represented by a combination of three operators $\mathcal{C}_{\mathbb{c},b} : \mathbb{I}_L \to \mathbb{I}_{\mathbb{c}}$, $CE : \mathbb{I}_{\mathbb{c}} \to \mathbb{I}_{\mathbb{c}}$, and $\mathcal{C}^{-1}_{\mathbb{c},b}(s) : \mathbb{I}_{\mathbb{c}} \to \mathbb{I}_L$:

$$CI_{b,c}(l) = \mathcal{C}^{-1}_{\mathbb{c},b}{}^{\circ} CE^{\circ} \mathcal{C}_{\mathbb{c},b} \text{ or } CI_{b,c}(l) = \mathcal{C}^{-1}_{\mathbb{c},b}(CE(\mathcal{C}_{\mathbb{c},b}(l))), \quad \text{for } l \in \mathbb{I}_L = [0, 1] \tag{11}$$

3.2. Construction of HA-based CI able to deal with expert LKBs

The main specific feature of the proposed method of the contrast intensification is its ability to deal with LKBs formulated by experts to change the contrast of a total given image (see for instance (12)), where $\mathcal{X}$ is the variable of the luminance of an original image, and $\mathcal{Y}$ is the variable of the luminance of its output image. As human beings are excellent at recognising reality in terms of their natural language, it seems to be very useful and practical to utilise experts' experience and knowledge of image quality enhancement. Thus, instead of trying to construct specific functions, e.g. power functions, as examined in [21,22], based on the researcher intuition, we may make use of the numeric function described by an LKB of an expert, e.g.

$$\begin{cases} (r1) \text{ If } \mathcal{X} \text{ is } \mathbf{0}, \text{ then } \mathcal{Y} \text{ is } \mathbf{0} \\ (r2) \text{ If } \mathcal{X} \text{ is } c^-, \text{ then } \mathcal{Y} \text{ is very } c^- \\ (r3) \text{ If } \mathcal{X} \text{ is } W, \text{ then } \mathcal{Y} \text{ is } W \\ (r4) \text{ If } \mathcal{X} \text{ is } c^+, \text{ then } \mathcal{Y} \text{ is very } c^+ \\ (r5) \text{ If } \mathcal{X} \text{ is } \mathbf{1}, \text{ then } \mathcal{Y} \text{ is } \mathbf{1} \end{cases} \tag{12}$$

In this section, we present how one can produce an S function to intensify the image contrast of a given image from a given expert LKB given in (12).

3.2.1. Definition of HA- based contrast intensification Hint

Let $\mathcal{AX} = (X, G_{\mathcal{X}}, H_{\mathcal{X}}, \le)$ and $\mathcal{AY} = (Y, G_{\mathcal{Y}}, H_{\mathcal{Y}}, \le)$ be HAs determined for the respective variables $\mathcal{X}$ and $\mathcal{Y}$ (at a given image pixel). Assume syntactically that $G_{\mathcal{X}} = G_{\mathcal{Y}} = \{c^-, c^+\}$, where $c^- = low$ and $c^+ = high$, $H_{\mathcal{X}} = H_{\mathcal{Y}} = \{little, very\}$; however, their quantitative semantics are different as they depend on their local image features. The independent fuzziness parameters of $\mathcal{X}$ are denoted by $fm_{\mathcal{X}}(c^-) = \theta_{\mathcal{X}}$ and $\mu(very) = \beta_{\mathcal{X}}$ and the ones of $\mathcal{Y}$ are denoted by $fm_{\mathcal{Y}}(c^-) = fm_{\mathcal{X}}(c^-) = \theta_{\mathcal{X}}$ and $\mu(very) = \beta_{\mathcal{Y}}$. Let $\mathfrak{v}_{\mathcal{X}}$ and $\mathfrak{v}_{\mathcal{Y}}$ be the SQMs of the respective variables $\mathcal{X}$ and $\mathcal{Y}$ determined by only giving their fuzziness parameter values; the rules in (12) are then transformed into five points in the space $[0, 1]^2$:

$$\left.\begin{array}{c} (\mathfrak{v}_{\mathcal{X}}(\mathbf{0}), \mathfrak{v}_{\mathcal{Y}}(\mathbf{0})), (\mathfrak{v}_{\mathcal{X}}(c^-), \mathfrak{v}_{\mathcal{Y}}(very\_c^-)), (\mathfrak{v}_{\mathcal{X}}(W), \mathfrak{v}_{\mathcal{Y}}(W)), \\ (\mathfrak{v}_{\mathcal{X}}(c^+), \mathfrak{v}_{\mathcal{Y}}(very\_c^+)) \text{ and } (\mathfrak{v}_{\mathcal{X}}(\mathbf{1}), \mathfrak{v}_{\mathcal{Y}}(\mathbf{1})) \end{array}\right\} \tag{13}$$

As $\mathfrak{v}_{\mathcal{X}}$ and $\mathfrak{v}_{\mathcal{Y}}$ preserve the order of their words, we have $\mathfrak{v}_{\mathcal{U}}(c^-) > \mathfrak{v}_{\mathcal{U}}(very\_c^-)$ and $\mathfrak{v}_{\mathcal{U}}(c^+) < \mathfrak{v}_{\mathcal{U}}(very\_c^+)$, because $c^- > very\_c^-$ and $c^+ < very\_c^+$, where the subscript $\mathcal{U}$ stands for either $\mathcal{X}$ or $\mathcal{Y}$.

These inequalities ensure that (13) approximately defines an S function.

Definition 1 (*Operator Hint*). Let HAs $\mathcal{AX}$ and $\mathcal{AY}$ and their semantic fuzziness parameters of the respective variables $\mathcal{X}$ and $\mathcal{Y}$ be described as above, noting that $\mathfrak{v}_{\mathcal{X}}(W) = \mathfrak{v}_{\mathcal{Y}}(W) = fm_{\mathcal{X}}(c^-) = \theta$. Then, an *HA CI*, denoted by *Hint*, described linguistically by (12), is understood as any continuous function that runs through the grid points given in (13), and it is also a contrast intensification with respect to $b = \mathfrak{v}_{\mathcal{X}}(W) = \theta$, i.e. it is a CI_{θ}.

3.2.2. Operator Hint determined by a given LKB and by a non-linear interpolation

To determine an appropriate CI defined by the LKB given in (12), by Definition 1, in general, we can apply any interpolation method (INTMd) to construct *Hint*, which is a function running through five points given in (13). In this study, we apply a non-linear interpolation method to produce *Hint* so that the contrast measurement of the luminance l' changed by *Hint* from the current luminance $l < b$ at a pixel, whose contrast measurement is $c_l = \mathcal{C}_{\mathbb{c},b}(l)$, is equal to $\mathcal{C}_{\mathbb{c},b}(l') = (c_l)^{\tau}$, for some exponent τ. Hence, $l' = Hint\ (l) = b\frac{1-(c_l)^{\tau}}{1+(c_l)^{\tau}}$.

To find an explicit non-linear expression of *Hint*, we need the following lemma to show that *Hint* enhances the image contrast better than a linear transformation, $T = \tau l$, for $l < b$, noting that the quantities $\left(\frac{1-a}{1+a}\right)^{\tau}$ and $\frac{1-\tau a}{1+\tau a}$ in the lemma are related to the image contrast measurements changed by *Hint* and *T*, respectively. The lemma will be applied to show that the image contrast changed by *Hint* is greater than the one changed by the method proposed in [21].

Lemma 1. *For* $\forall a \in (0, 1)$ *and* $\forall \tau \in (0, 1)$, *we always have*

(i) $\left(\frac{1-a}{1+a}\right)^{\tau} < \frac{1-\tau a}{1+\tau a}$

(ii) For $\forall a \in (0, 1)$ *and* $\forall \tau \in (0, 1)$, *we have*

(a) There exists $\gamma = \gamma(a, \tau) \in (0, 1)$ *such that* $\left(\frac{1-a}{1+a}\right)^{\gamma} = \frac{1-\tau a}{1+\tau a}$ *and* $\gamma = \gamma(a, \tau) < \tau$

(b) $\left(\frac{1-l}{1+l}\right)^{\gamma} < \frac{1-\tau l}{1+\tau l}$, *for all l such that* $a < l \le 1$, *and* $\frac{1-\tau l}{1+\tau l} < \left(\frac{1-l}{1+l}\right)^{\gamma} < \frac{1-\gamma l}{1+\gamma l}$, *for all l such that* $0 < l < a$.

Proof. See Appendix A.

To construct a suitable *Hint*, we introduce a parameter m that satisfies the condition,

$$m = \frac{\mathfrak{v}^2_{\mathcal{Y}}(very\_low)}{\mathfrak{v}_{\mathcal{X}}(low)} = \frac{\beta^2_{\mathcal{Y}}}{\beta_{\mathcal{X}}} \tag{14}$$

to control the degree of the contrast intensification defined by the LKB in (12), where the second equality in (14) is deduced from (5), and hence, $\beta_{\mathcal{Y}} = \sqrt{m\beta_{\mathcal{X}}}$. Because the order-based structure of every HA of $\mathcal{X}$ is symmetric to W [48,60] in the sense that for every string of hedges $\sigma = h_k \ldots h_1, h_j \in H, \sigma c^{\epsilon} \le W$ iff $\sigma c^{-\epsilon} \ge W$, where

$\epsilon, -\epsilon \in \{-, +\}$; then, for any function $\phi(fm(c^{-\epsilon}), \beta_{\mathcal{X}})$ defined by the fuzziness parameters of $\mathcal{X}$, we have

$$\mathfrak{v}_{\mathcal{X}}(\sigma c^{-\epsilon}) = \phi(fm(c^{-\epsilon}), \beta_{\mathcal{X}}) \text{ iff } \mathfrak{v}_{\mathcal{X}}(\sigma c^{\epsilon}) = 1-\phi(1-fm(c^{-\epsilon}), \beta_{\mathcal{X}}) \tag{15}$$

For instance, by (5), we have $\mathfrak{v}_{\mathcal{X}}(Vc^-) = \beta_{\mathcal{Y}}^2 fm(c^-)$. By (15), it implies that $\mathfrak{v}_{\mathcal{X}}(Vc^+) = 1 - \beta_{\mathcal{Y}}^2(1 - fm(c^-))$, which is just the SQM value of the word Vc^+ computed by (5). This suggests us to define a concept of a θ-*sym function* (θ-*sym* : means *symmetric* to θ) with parameter $\theta = fm(c^-)$ as follows: $\Phi(l, \theta) : [0, 1] \to [0, \theta]$ is said to be θ-symmetric, provided that, for $\forall l \in [\theta, 1]$, $\Phi(l, \theta) = 1 - \Phi(1 - l, 1 - \theta)$, and hence, for $\forall l \in [0, \theta]$, we have $\Phi(l, \theta) = 1 - \Phi(1 - l, 1 - \theta)$. Put $\bar{\theta} = 1 - \theta$ and $\bar{l} = 1 - l$, we have the following θ-*sym* rule, R_θ, for any θ-*sym* function $\Phi(l, \theta)$:

$$\Phi_{[0,\theta]}(l, \theta) = b, \text{ for } l \in [0, \theta] \Leftrightarrow \Phi_{[\theta,1]}(\bar{l}, \bar{\theta}) = R_\theta(\Phi_{[0,\theta]}(l, \theta)) = 1-b, \text{ for } \bar{l} \in [\theta, 1] \tag{16}$$

It can be verified that SQMs of HAs are θ-symmetric functions. Thus, for a θ-*sym* function Φ, it is necessary to define or calculate it in one of the intervals $[0, \theta]$ or $(\theta, 1]$.

We first define the contrast intensificator CI_b on $[0, \theta]$, for $b = \theta_{\mathcal{X}}$ ($= \theta$, for short), as follows:

$$\mathcal{C}_{\mathfrak{c},\theta}(l) = \frac{|l - \theta|}{l + \theta}, \; CE = (.)^\gamma, \text{ i.e. } CE(s) = s^\gamma,$$

$$\text{where } \gamma = \gamma(\theta, m) = \ln\left(\frac{1 - m\theta}{1 + m\theta}\right) \Big/ \ln\left(\frac{1 - \theta}{1 + \theta}\right).$$

That is, $CE(\mathcal{C}_{\mathfrak{c},\theta}(l)) = \left(\frac{|l-\theta|}{l+\theta}\right)^\gamma$. On the interval $(1 - \theta, 1]$, CE is obtained by rule R_θ, i.e.

$$\mathcal{C}_{\mathfrak{c},\theta}(l) = R_\theta(\mathcal{C}_{\mathfrak{c},\theta}(l)) = \frac{l - \theta}{2 - (l + \theta)}, \; CE(\mathcal{C}_{\mathfrak{c},\theta}(l)) = \left(\frac{l - \theta}{2 - (l + \theta)}\right)^\gamma, \text{ for } l \in (\theta, 1] \tag{17}$$

Utilising the θ-*sym* rule R_θ, it is only necessary now to define $Hint_\theta$ on the interval $[0, \theta]$. Because, by Lemma 1, $\gamma(\theta, m) < m \in (0, 1)$, obviously we have $CE(c) = (c)^\gamma \geq c$, $c \in \mathbb{I}_{\mathfrak{c}}$, and hence, it is a contrast enhancement operator defined by (9). With such specific features, this CI, denoted by $Hint_\theta$, can be written as follows:

$$Hint_\theta = \mathcal{C}_{\mathfrak{c},\theta}^{-1} \circ CE \circ \mathcal{C}_{\mathfrak{c},\theta}, \text{ noting that } \mathcal{C}_{\mathfrak{c},\theta}^{-1}\left(\frac{|l - \theta|}{l + \theta}\right) = l, \text{ for all } l \in [0, \theta] \tag{18}$$

$$\text{or } Hint_\theta(l) = \mathcal{C}_{\mathfrak{c},\theta}^{-1}\left(\mathcal{C}_{\mathfrak{c},\theta}(l)\right)^\gamma = \mathcal{C}_{\mathfrak{c},\theta}^{-1}\left(CE(\mathcal{C}_{\mathfrak{c},\theta}(l))\right) \text{ and } \mathcal{C}_{\mathfrak{c},\theta}(Hint_\theta(l)) = CE(\mathcal{C}_{\mathfrak{c},\theta}(l)) \tag{19}$$

Thus, (19) states that $Hint_\theta$ is computed by means of the contrast enhancement operator CE defined by using an exponential function and the contrast measure operator $\mathcal{C}_{\mathfrak{c},\theta}$; hence, the explicit expression of $Hint_\theta$ can be easily established together with its properties as follows:

Theorem 1. *For a given LKB $\mathcal{K}b$, let the assumptions on the semantics of $\mathcal{AX}$ and $\mathcal{AY}$ of the luminance linguistic variables be the same as those given in Definition 1 and the parameters $\beta_{\mathcal{X}}$, $\beta_{\mathcal{Y}}$, and m be satisfied by (14). Then, $Hint_\theta$ defined by (18)* and *(19) has the following properties:*

(i) $Hint_\theta$ is a CI, which is explicitly represented by

$$Hint_\theta(l) = \begin{cases} \theta\frac{1-CE(\mathcal{C}_{\mathfrak{c},\theta}(l))}{1+CE(\mathcal{C}_{\mathfrak{c},\theta}(l))} & \text{for } 0 < l \leq \theta \\ 1 - (1 - \theta)\frac{1-CE(\mathcal{C}_{\mathfrak{c},\theta}(l))}{1+CE(\mathcal{C}_{\mathfrak{c},\theta}(l))} & \text{for } \theta < l \leq 1 \end{cases} \tag{20}$$

where $\gamma = \gamma(\beta_{\mathcal{X}}, m) = \ln\left(\frac{1-m\beta_{\mathcal{X}}}{1+m\beta_{\mathcal{X}}}\right) / \ln\left(\frac{1-\beta_{\mathcal{X}}}{1+\beta_{\mathcal{X}}}\right)$.

(ii) $Hint_\theta$ defines a non-linear interpolation method, i.e. it runs through the points given in (13) produced by the LKB in (12), that is, $Hint_\theta(l) = INTMd_{(\mathcal{K}b, Hint\theta)}(l)$. Moreover, we have

$$\max_{l\in(0,\mathfrak{v}_{\mathcal{X}}(c^-))} \frac{Hint_\theta(l)}{l} = \min_{l\in(\mathfrak{v}_{\mathcal{X}}(c^-),\theta)} \frac{Hint_\theta(l)}{l} = \max_{l\in(\theta,\mathfrak{v}_{\mathcal{X}}(c^+))} \frac{1 - Hint_{\bar{\theta}}(l)}{1 - l} = \min_{l\in(\mathfrak{v}_{\mathcal{X}}(c^+),1)} \frac{1 - Hint_{\bar{\theta}}(1 - l)}{1 - l} = m$$

Proof. See Appendix B.

Because it will be seen that the proposed method is more effective than the methods proposed by Cheng et al. [21,22], it is useful to expose its following specific properties, which are different from their corresponding contrast enhancement operator CE_{Ch} and contrast intensificator CI_{Ch}.

Theorem 2. *Let $\mathcal{AX}$ and $\mathcal{AY}$ be HAs with the same assumptions as given in Theorem 1, where the fuzziness parameters of $\mathcal{AX}$ are $\mu(Very_{\mathcal{X}}) = \beta_{\mathcal{X}} = \beta$ and $fm(c^-) = \theta$. Assume also that the parameter m is equal to ξ, defined in [21]. Then, $Hint_\theta$ has also the following features:*

(i) The contrast enhancement produced by CE_θ of $Hint_\theta$ is larger than the one produced by CE_{Ch} of CI_{Ch} proposed in [21], i.e. we have $CE_\theta = \left(\mathcal{C}_{\mathfrak{c},\theta}(l)\right)^\gamma > CE_{Ch} = \left(\mathcal{C}_{\mathfrak{c},\theta}(l)\right)^{\xi^t}$, for $t \in [0, 1]$, noting that the contrast measure operator $\mathcal{C}_{\mathfrak{c},\theta}$ of $Hint_\theta$ and the one of CI_{Ch} are the same.

(ii) In the luminance interval $\Im\left(Vc^-\right) = [0, \mathfrak{v}_{\mathcal{X}}\left(c^-\right)]$, which represents an interval semantics of Vc^- = 'very_low', $Hint_\theta$ intensifies the image contrast better than CI_{Ch} does, i.e. we have, for $\forall l \in \Im\left(Vc^-\right) = [0, \mathfrak{v}_{\mathcal{X}}\left(c^-\right)]$, $Hint_\theta(l) < \mathcal{C}_{\mathfrak{c},\theta}^{-1}(CE_{Ch}(\mathcal{C}_{\mathfrak{c},\theta}(l))) = CI_{Ch}(l)$.

Proof. See Appendix C.

Remarks. Because the fuzziness parameter values of $\theta_{\mathcal{X}}$ and $\theta_{\mathcal{Y}}$ are equal, i.e. the semantics intervals of the word *low* $= c^-$ of $\mathcal{X}$ and $\mathcal{Y}$ are identical, the inequality in (ii) means that the region of luminance of the output image (the variable $\mathcal{Y}$) linguistically described by *very_low* produced by $Hint_\theta$ is greatly reduced compared to that produced by CI_{Ch}. Consequently, the semantics interval of the word *little low* produced by $Hint_\theta$ is larger than that produced by CI_{Ch}.

In fact, as aforementioned, because the structure of HAs is symmetric to the neutral word W lying in between c^- and c^+, which corresponds to the numeric value θ in the normalised domain [0,1], it is required that $Hint_\theta$ is θ symmetric, and hence, $Hint_\theta$ on the interval $[\theta, 1]$ can be computed from $Hint_\theta$ defined in $[0, \theta]$ by applying the θ rule. It is different from the way the operator CI_{Ch} is defined by (21) given below, in which δ plays the role of θ, where CI_{Ch} is not required to satisfy the δ-symmetric rule. In addition, using this formula to compute the values of CI_{Ch} in $[\delta, 1]$, there are numerous values of CI_{Ch} beyond its normalised range [0, 1]. In fact, assume that the range of luminance values of CI_{Ch} is normalised to be [0, 1]. By its definition,

$$CI_{Ch}(l) = \begin{cases} \delta\frac{1-C_{\mathfrak{c},\delta}(l)^{\xi^t}}{1+C_{\mathfrak{c},\delta}(l)^{\xi^t}} & \text{for } l \leq \delta \\ \delta\frac{1+C_{\mathfrak{c},\delta}(l)^{\xi^t}}{1-C_{\mathfrak{c},\delta}(l)^{\xi^t}} & \text{for } l > \delta \end{cases} \tag{21}$$

Clearly, we have $C_{\mathfrak{c},\delta}(\delta)^{\xi^t} = 0$ and $C_{\mathfrak{c},\delta}(1)^{\xi^t} = \left(\frac{1-\delta}{1+\delta}\right)^{\xi^t} > \frac{1-\theta}{1+\theta}$ on the interval $[\delta, 1]$. It follows that there exists an $l_0 \in (0, 1)$ such that $C_{\mathbb{c},\delta}(l_0)^{\xi^t} = \frac{1-\delta}{1+\delta}$, which implies by the increasing monotonicity of $C_{\mathbb{c},\delta}(l)^{\xi^t}$ that, for $\forall l \in (l_0, l)$, $C_{\mathbb{c},\delta}(l)^{\xi^t} > C_{\mathbb{c},\delta}(l_0)^{\xi^t}$. Thus, by (21), for $\forall l \in (l_0, l)$, we have $CI_{Ch}(l) = \delta \frac{1+C_{\mathbb{c},\delta}(l)^{\xi^t}}{1-C_{\mathbb{c},\delta}(l)^{\xi^t}} > \delta \frac{1+C_{\mathbb{c},\delta}(l_0)^{\xi^t}}{1-C_{\mathbb{c},\delta}(l_0)^{\xi^t}} = \delta \frac{1+\frac{1-\delta}{1+\delta}}{1-\frac{1-\delta}{1+\delta}} = 1$, which is what we expect.

4. Proposed method of image contrast intensification

In this section, for a given raw multichannel image $\mathbb{i}$, we present how one can construct an image *CI* on a formal basis presented in Sections 2 and 3. It is different from the image *CI*s in the indirect approach that deal with image histograms. The image *CI*s examined in this study deal directly with the luminance at each pixel, i.e., the *atomic* elements of the image. Therefore, the proposed method will be constructed based on a perspective that it must preserve the global image features as well as local details of $\mathbb{i}$ when changing the luminance at pixel level. Thus, it is developed to achieve a balanced combination between (i) the operator *Hint*, which is defined by (12)–(20) in Section 3, to utilise the inherent semantics of LKB expressed by a human expert based on his/her global view of multichannel images but applied to individual pixels of each image channel and (ii) a standard FCM, $\mathfrak{C}_{fz}$, applied to the entire multichannel $\mathbb{i}$. The first-time application of human user's LKB and the FCM of the proposed method makes it different from the existing methods in this field. Note that when *Hint* deals with an LKB formulated for the entire $\mathbb{i}$, it may preserve certain global image features. However, when dealing with the luminance at each image pixel of every channel, it may lose image details. Thus, before *Hint* is applied to the individual channels of $\mathbb{i}$, the FCM $\mathfrak{C}_{fz}$ is utilised to divide the whole $\mathbb{i}$ into fuzzy clusters to reveal useful global features derived from the similarity of the pixel luminance of $\mathbb{i}$. Then, a fuzzificator F_k of $\mathbb{i}_k$, which is the projection of $\mathbb{i}$ on each k channel, is formed by an aggregation of the natural fuzzificators of its clusters projected on the k channel to capture the revealed cluster features. Now, *Hint* is applied to $F_k(\mathbb{i}_k)$ instead of $\mathbb{i}_k$. Thus, as each luminance l_{ij} of a pixel p_{ij} of $\mathbb{i}$ belongs to every fuzzy cluster with its weight, *Hint* may maintain the global features of the fuzzy clusters when changing $F_k(l_{ij})$.

4.1. General description of how to construct an image CI

As previously mentioned, any image $\mathbb{i}$ of K channels can be identified with a mapping-vector $\mathbb{i} = (\mathbb{i}_1, \ldots, \mathbb{i}_\kappa)$, where $\mathbb{i}_k : \{p_{i,j} : i = 1 \text{ to } M \text{ and } j = 1 \text{ to } N\} \rightarrow [L_{k,min}, L_{k,max}]$, which is identified with the k-channel $\mathbb{i}_k$ of $\mathbb{i}$. The luminance of each pixel $p_{i,j}$ of $\mathbb{i}$ is then represented as a vector $\vec{l}_{ij} = (l_{ij,1}, \ldots, l_{ij,K})$, where $l_{k,ij} = \mathbb{i}_k(p_{ij}) \in [L_{k,\min}, L_{k,\max}]$, and we can write it as $\mathbb{i} = \{\mathbb{i}(i,j) = \vec{l}_{ij}$, for $1 \le i \le M$ and $1 \le j \le N\}$.

As LKB is a distinguished feature of the proposed method, to make use of human expert capabilities to construct the operator *Hint* acting on a given input $\mathbb{i}$, the following main tasks must be done including the determination of the syntax and semantics of variables $\mathcal{X}$ and $\mathcal{Y}$:

Task 1. Define the syntactical semantics of variables $\mathcal{X}$ *and* $\mathcal{Y}$ *of* $\mathbb{i}$. It is required to determine which hedges are suitable for $\mathbb{i}$. For the syntactic semantics of $\mathcal{X}$ and $\mathcal{Y}$, it is necessary only to determine the negative and positive hedges and their relative signs to form a table similar to Table 1. In this study, one negative and one positive hedge are sufficient to show the performance of the constructed *Hint*. The syntactic semantics of a variable depends strongly on which hedges are used. For example, assume that either $H = \{R, V\}$ or $H' = \{L, V\}$, whose hedges are selected from a natural language, is applied for $\mathcal{X}$. The syntactic semantics of $\mathcal{X}$ defined by either H or H' is relatively different, as shown by comparing the relative signs of their hedges determined in Tables 2 and 3. Thus, which syntactic semantics of a variable is suitable for $\mathbb{i}$ depends on the experience of the expert in rendering his/her LKB. When the syntactic semantics of $\mathcal{X}$ and $\mathcal{Y}$ is defined, the expert may formulate his/her LKB $\mathcal{B}$ to change the luminance, say

Table 2
Relative sign of a hedge of H in a row with respect to a hedge in a column.

$sign(h, k)$	V	R
V	+	−
R	−	+

Table 3
Relative sign of a hedge of H' in a row with respect to a hedge in a column.

$sign(h, k)$	V	L
V	+	+
L	−	−

$$\mathcal{B} = \{\text{Rule } r_i := \text{ If } \mathcal{X} \text{ is } x_i \text{ then } \mathcal{Y} \text{ is } y_i : x_i \in \mathrm{Dom}(\mathcal{X}) \text{ and } y_i \in \mathrm{Dom}(\mathcal{Y}), i = 1 \text{ to } n\}$$

which in the field of image contrast intensification, must always be increasing, i.e. it defines an increasing linguistic function.

Task 2. Determine the quantitative semantics of $\mathcal{X}$ *and* $\mathcal{Y}$ *at each image pixel* p_{ij}. It is necessary to provide only suitable numeric values of the fuzziness parameters of the variables. These values are determined based on two main requirements: (i) to capture the inherent semantics of words, i.e. they at least satisfy constraints (1) and (2) in Section 2; (ii) to capture local features of $\mathbb{i}$ at each image pixel p_{ij}. In this study, the numeric semantics of W or the SQM value $\theta = fm(c^-)$ of W and the fuzziness parameter $\beta_{\mathcal{Y}}$ related to the fuzziness measure of the hedges of $\mathcal{Y}$ of the output-image luminance should be determined in close relation to the image characteristics at p_{ij}. For instance, in this study, θ may be defined by the surrounding luminance b_{ij} of p_{ij}, and $\beta_{\mathcal{Y}}$ of the k channel is defined by $\beta_{\mathcal{Y}_{k,ij}} = \sqrt{\xi_{k,ij}\beta_{\mathcal{X}_{k,ij}}}$, where $\xi_{k,ij}$ is Cheng's local feature [21]. It is advantageous that, for a given syntactic semantics of a variable, when its fuzziness parameter values are provided, the compt.-semantics of all words of the variable can be calculated, even if they are potentially infinite, as discussed in Section 2, whereas in the fuzzy set-based approaches, the fuzzy sets of the words in question are individually constructed by experts. When an additional word is required, the fuzzy sets constructed for the old words must be reconstructed.

Task 3. Determine a method of computing the S function described by the expert's LKB. Transform the expert's LKB $\mathcal{B}$ representing an increasing linguistic function defined on the words of $\mathcal{X}$ present in $\mathcal{B}$ into a grid of points in the Euclidean space $[0, 1]^2$; then, compute a numeric S function going through the points of the grid that represents a desired image *CI*.

- As discussed in Section 2, Point 2.2.1, and Example 1, when providing the fuzziness parameter values of each variable $\mathcal{X}$ or $\mathcal{Y}$, it is easy to compute the numeric semantics (i.e. the values of SQMs $\mathfrak{v}_{\mathcal{X}}$ and $\mathfrak{v}_{\mathcal{Y}}$) of their words. The LKB $\mathcal{B}$ considered as defining n linguistic points (x_i, y_i), $i = 1$ to n, can be transformed into a grid $\mathcal{G}$ of n points $(\mathfrak{v}_{\mathcal{X}}(x_i), \mathfrak{v}_{\mathcal{Y}}(y_i))$'s in $[0, 1]^2$, while preserving the semantic order of the words.
- Apply a suitable interpolation method preserving the monotonicity of $\mathcal{B}$ to the grid $\mathcal{G}$ to produce an S function of the desired *CI*. For example, *Hint* examined in Section 3 is constructed by an interpolation using a non-linear increasing function defined by (20).

4.2. Keeping a balance of global image features and its local details by using FCM $\mathfrak{C}_{fz}$

As mentioned above, the operator *Hint* is constructed based on utilising a given LKB $\mathcal{B}$, interpreted as representing a global feature, because it is formulated based on a global expert's view of the given image $\mathfrak{i}$, although it is applied at each image pixel. This is a way to achieve the balance mentioned above. To enhance this balance, a proposed method is developed to combine the operator *Hint* and a standard FCM, $\mathfrak{C}_{fz}$, applied to the whole image to reveal some of their useful global features, which can be deduced from the similarity of the pixel luminance values of $\mathfrak{i}$.

The idea of combining *Hint* with the FCM $\mathfrak{C}_{fz}$ is realised as follows. Assume that $\mathfrak{i}$ is decomposed into C fuzzy clusters by $\mathfrak{C}_{fz}$. These fuzzy clusters are projected to each channel $\mathfrak{i}_k$. Then, compute the fuzzy histogram of each projected cluster and its dynamic range $[B_{ck1}, B_{ck2}] \subseteq [L_{k,\min}, L_{k,\max}]$. Now, the fuzzified luminance l of the given image $\mathfrak{i}$ projected to $\mathfrak{i}_k$ is computed by

$$F_k(l) = \frac{\sum_{c=1}^{C} min\left\{max\left\{\frac{l-B_{ck1}}{B_{ck2}-B_{ck1}}, 0\right\}, 1\right\}}{C} \in [0, 1] \tag{22}$$

where $F_k(l)$ is the normalised luminance value of $\mathfrak{i}'_k$ of $\mathfrak{i}_k$, i.e. the projection of $\mathfrak{i}$ to $\mathfrak{i}_k$. The operator *Hint* is now applied to $\mathfrak{i}'_k$ instead of $\mathfrak{i}_k$. In this way, the proposed method may preserve the global cluster feature revealed by the FCM applied to the whole image $\mathfrak{i}$.

4.3. Algorithm of image contrast intensification based on the proposed method

The image *CI Hint* is developed by utilising an LKB $\mathcal{B}$ formulated by an expert based on a global view of an entire given image but is applied to change the luminance at each pixel of the image $\mathfrak{i}_k$, where $k = 1$ to K. Therefore, the fuzziness parameter values of the linguistic variables $\mathcal{X}$ and $\mathcal{Y}$ to compute the numeric semantics of $\mathcal{B}$ are pixel-dependent, and hence, must be determined at each pixel, as discussed in Section 4.1. In this algorithm, they are determined as follows to utilise specific local features of the image at each pixel p_{ij}, using two local features $\delta'_{k,ij}$ and $\xi_{k,ij}$, where $\xi_{k,ij}$ is Cheng's amplification constant [21] while $\delta'_{k,ij}$ is defined similarly as Cheng's feature $\delta_{k,ij}$, the mean non-homogeneity grey value for a specified window, but the local homogeneity measurement examined in [21] is redefined by using nanother aggregation operator as examined in Section 5.1.1: Assume $fm\left(c^-_{\mathcal{X}}\right) = fm(c^-_{\mathcal{Y}}) = \theta$; then, put $\theta = \delta'_{k,ij}(F_k(\mathfrak{i}_k))$, $\beta_{\mathcal{X}} = 0.6$, and $\beta_{\mathcal{Y}} = (0.6{*}\xi_{k,ij})^{1/2}$. When these fuzziness parameters are determined as such, *Hint* is completely defined.

For an image $\mathfrak{i} = (\mathfrak{i}_1, \ldots, \mathfrak{i}_K)$ having K channels, before *Hint* is applied to $\mathfrak{i}$, it is divided into C clusters, for a given integer C, by applying a standard FCM. It computes C centres of the clusters, $\vec{v}_c = (v_{c1}, \ldots, v_{cK})$, and membership degrees $\mu_{c,ij}$ of every luminance vector $\vec{l}_{ij} = (l_{1,ij}, \ldots, l_{K,ij})$ to the c-th cluster with the kernel $\vec{v}_c$, for $c = 1$ to C, where $1 \le i \le M$ and $1 \le j \le N$, using the following objective function:

$$J(v, \mu) = \sum_{i,j=1}^{n}\sum_{c=1}^{C}\mu_{c,ij}^{p} D\left(\vec{v}_c, \vec{l}_{ij}\right)^2 = \sum_{i,j=1}^{n}\sum_{c=1}^{C}\mu_{c,ij}^{p}\sum_{k=1}^{K}(v_{c,k} - l_{ij,k})^2 \to min$$

subject to

$$\begin{cases} \mu_{c,ij} \in [0, 1], \text{for } \forall i,\ j \text{ and } \forall c\colon 1 \le c \le C \\ \sum_{c=1}^{C}\mu_{c,ij} = 1, \text{for } \forall i, j \\ \sum_{i,j}\mu_{c,ij} > 0,\ \forall c\colon 1 \le c \le C \end{cases} \tag{23}$$

where the parameter $p > 0$ is specified as 2. Thus, for every cluster c, the image $\mathfrak{i}$ is associated with an indexed set $\{(\vec{l}_{ij}, \mu_{c,ij}) : 1 \le i \le M \text{ and } 1 \le j \le N\}$.

For k, $1 \le k \le K$, and any $l_k \in [L_{k,\min}, L_{k,\max}]$, putting $\mathrm{Pr}_k(l_{ij,1}, \ldots, l_{ij,K}) = l_{ij,k}$ and $\mathfrak{i}_k^{-1}(l_k) = \{(i, j) : \mathrm{Pr}_k(\mathfrak{i}(i, j)) = l_k\}$, the fuzzy histogram of $\mathfrak{i}_k$ is defined as follows:

$$\mathfrak{h}_{ck}(l_k) = \sum_{(i,j)\in \mathfrak{i}_k^{-1}(l_k)} \mu_{c,ij} \in [0, MN] \tag{24}$$

Proposed algorithm *Hint-F*$\mathfrak{C}_{fz}$

Input:

- A K-channel image $\mathfrak{i}$ with the luminance domain of each k-channel $\mathfrak{i}_k$ being $[L_{k,min}, L_{k,max}]$;
- An LKB $\mathcal{K}b$ associated with two HAs $\mathcal{AX}$ (of $\mathfrak{i}$) and $\mathcal{AY}$ (of the output of $\mathfrak{i}'$) with their specified syntactic semantics and the specified fuzziness parameter $\beta = \mu(Very_{\mathcal{X}})$ of $\mathcal{AX}$ of only the input variable $\mathcal{X}$, in which both are commonly applied to all pixels p_{ij}*'s* of $\mathfrak{i}$;
- Parameter d, which is the size of the window at each pixel, $d \times d$;
- C, which is the number of clusters of $\mathfrak{C}_{fz}$;

Output: The contrast-enhanced image $\mathfrak{i}'$ of $\mathfrak{i}$, $\mathfrak{i}'$ = Output($\mathfrak{i}$)

For each pixel p_{ij}

For each $\mathfrak{i}_k = \{\mathfrak{i}_k(p_{i,j}) \in [L_{k,min}, L_{k,max}] : i = 1 \text{ to } M \text{ and } j = 1 \text{ to } N\}$, $1 \le k \le K$,

Step 1. Construct a fuzzificator for every $\mathfrak{i}_k$ based on the standard FCM, $\mathfrak{C}_{fz}$, of the whole image $\mathfrak{i}$:

1.1. Cluster the whole image $\mathfrak{i}$ into C fuzzy clusters that produce C arrays, $c = \{(\vec{l}_{ij}, \mu_{c,ij}) : 1 \le i \le M \text{ and } 1 \le j \le N\}$, for $c = 1$ to C.

1.2. For each $k = 1$ to K , compute a fuzzy histogram $\mathfrak{h}_{ck} : [L_{k,\min}, L_{k,\max}] \to [0, MN]$ using (24).

1.3. Compute a dynamic range of grey levels of $\mathfrak{i}_k$ for every cluster c: for any $c = 1$ to C, compute parameters B_{ck1} and B_{ck2} using the following formulas (25):

$$\begin{rcases} B_{ck1} = \underset{L_{k,min}\le B\le L_{k,max}}{arg\ min}\left\{\sum_{l=L_{k,min}}^{B}\mathfrak{h}_{ck}(l) \ge f * \sum_{l=L_{k,min}}^{L_{k,max}}\mathfrak{h}_{ck}(l)\right\} \\ B_{ck2} = \underset{L_{k,min}\le B\le L_{k,max}}{arg\ max}\left\{\sum_{l=B}^{L_{k,max}}\mathfrak{h}_{ck}(l) \ge f * \sum_{l=L_{k,min}}^{L_{k,max}}\mathfrak{h}_{ck}(l)\right\} \end{rcases} \tag{25}$$

where f is a parameter. Note that B_{ck1} and B_{ck2} are determined from the fuzzy clusters produced by $\mathfrak{C}_{fz}$ projected on the k channel. This establishes a method of relating K channels $\mathfrak{i}_1, \ldots, \mathfrak{i}_K$ of $\mathfrak{i}$ to each other as indicated in (22).

1.4. Construct a fuzzificator F_k of $\mathfrak{i}_k$, $F_k : \mathfrak{i}_k \to [0, 1]$, $k = 1$ to K as follows: for every pixel $p_{i,j}$ with luminance $l_{ij} \in [L_{k,\min}, L_{k,\max}]$, compute $F_k(l)$ using (22) and (25).

Step 2.

2.1. Compute Cheng's parameters characterising specific local features at each pixel based on the ordinary histogram $\mathfrak{H}_k$ of $F_k(\mathfrak{i}_k)$.

2.2. Compute the array of the mean non-homogeneity grey values $\delta_{k,ij}$ of the windows of size $d \times d$ surrounding each of $M \times N$ pixels of $F_k(\mathfrak{i}_k)$.

2.3. Compute the pixel contrast amplification constants $\xi_{k,ij}$.

Step 3. Compute $Hint_\theta(l_{k,ij})$ by applying the reasoning method INTMd$_{(\mathcal{K}b,Hint\theta)}$ (see Theorem 1)

3.1. Determine suitable values of independent fuzziness parameters of $\mathcal{AX}$ and $\mathcal{AY}$ at p_{ij}:

$fm_k(c^-) = \theta_{k,ij} = \delta_{k,ij}(F_k(\mathfrak{i}_k))$, $\beta_{\mathcal{X},ij} = \beta$ (the input parameter), $m = \xi_{k,ij}$, and $\beta_{\mathcal{Y},ij} = \sqrt{\beta m}$.

3.2. Calculate amplification constant, $\gamma_{k,ij} = \frac{\log\left(\frac{1-\beta\xi_{k,ij}}{1+\beta\xi_{k,ij}}\right)}{\log\left(\frac{1-\beta}{1+\beta}\right)}$.

3.3. Compute the contrast enhancement operator CE at pixel p_{ij} of $F_k(\mathfrak{i}_k)$:

3.3.1. Putting $\hat{l}_{k,ij} = F_{k,ij}\left(l_{k,ij}\right)$, compute its contrast $C_{\mathbb{c},b}$, where $b = \theta_{k,ij}$, at pixel p_{ij}

$$C_{\mathbb{c},\theta_{k,ij}}\left(\hat{l}_{k,ij}\right) = \begin{cases} \frac{\theta_{k,ij}-\hat{l}_{k,ij}}{\theta_{k,ij}+\hat{l}_{k,ij}} & \text{for } 0 \le \hat{l}_{k,ij} \le \theta_{k,ij} \\ \frac{\hat{l}_{k,ij}-\theta_{k,ij}}{2-(\theta_{k,ij}+\hat{l}_{k,ij})} & \text{for } \theta_{k,ij} < \hat{l}_{k,ij} \le 1 \end{cases}$$

3.3.2. Compute $CE\left(C_{\mathbb{c},\theta_{k,ij}}\left(F_{k,ij}\left(l_{k,ij}\right)\right)\right) = \left(C_{\mathbb{c},\theta_{k,ij}}\left(F_{k,ij}\left(l_{k,ij}\right)\right)\right)^{\gamma_{k,ij}} \in [0, 1]$.

3.4. Compute the value $Hint_\theta(l_{k,ij})$: based on Theorem 1, where $Hint_\theta = \mathcal{C}_{\mathbb{c},\theta}^{-1} \circ CE \circ \mathcal{C}_{\mathbb{c},\theta}$.

Step 4. Compute the luminance $l'_{k,ij}$ value at p_{ij} of the output F'_k of $F_k(\mathfrak{i}_k)$:

$$4.1.\ l^F_{k,ij} = \begin{cases} \theta_{k,ij}\frac{1-CE\left(\mathcal{C}_{\mathbb{c},\theta_{k,ij}}\left(\hat{l}_{k,ij}\right)\right)}{1+CE\left(\mathcal{C}_{\mathbb{c},\theta_{k,ij}}\left(\hat{l}_{k,ij}\right)\right)} & \text{for } 0 \le \hat{l}_{k,ij} \le \theta_{k,ij} \\ 1-(1-\theta)\frac{1-CE\left(\mathcal{C}_{\mathbb{c},\theta_{k,ij}}\left(\hat{l}_{k,ij}\right)\right)}{1+CE\left(\mathcal{C}_{\mathbb{c},\theta_{k,ij}}\left(\hat{l}_{k,ij}\right)\right)} & \text{for } \theta_{k,ij} \le \hat{l}_{k,ij} \le 1 \end{cases},$$

where $l^F_{k,ij} \in F'_k$.

4.2. $l'_{k,ij} = F_k^{-1}\left(l^F_{k,ij}\right) = \max_{1\le c\le C}\{B_{ck2} - B_{ck1}\}\,\hat{l}_{k,ij} + \frac{\sum_{c=1}^{C} B_{ck1}}{C}$

End For each $\mathfrak{i}_k$, $1 \le k \le K$.

End For each pixel p_{ij},

Return the output image i'.

We must emphasise that, according to our knowledge, the fuzzy clustering technique is for the first time applied to fuzzify channel images in this topic to exploit regional features of the fuzzy regions defined by fuzzy clusters. As the applied FCM works on a whole multichannel image, each obtained fuzzy cluster c determines K fuzzy clusters c_k's projected on their respective K channels. Hence, the fuzzificators F_k's defined in Step 1 are dependent from each other and they can exploit local features of the fuzzy regions c_k, $c = 1, \ldots, C$, for every k. Similarly, the parameters B_{ck1} and B_{ck2} computed using the fuzzy histograms $\mathfrak{h}_{ck}$ are examples of exploiting local features of the components c_k's in the context of the whole fuzzy region c. This technique may maintain certain dependence between the image channels in representing image details, whilst a balance between global features and local ones of the input image can be reached.

5. Experiments

Because the proposed method is composed of three components, namely the operator *Hint*, a homogeneity measurement HO_{MP} improved from the one proposed in [21], HO_{Ch03}, and the FCM $F\mathfrak{C}_{fz}$, the intended experiments are organised, first, to show the efficacy of the individual proposed components, and second, to show the effective performance of the proposed method *Hint*-$F\mathfrak{C}_{fz}$ using the surrounding luminance defined from HO_{MP}. The experimental data for the first objective are the six images shown in Fig. 4, which seem to be sufficient for examination of the functionality of the proposed components. For the second objective, 27 images are taken as inputs consisting of the ones shown in Fig. 4 merged with 24 of 25 images of image database TID2013 [63] except for its unique one, which is artificially made. To attain these objectives, the following four experiments will be performed:

Exp1. To show the outperformance of *Hint* over Ch_{03} using the same contrast definition.

Exp2. To examine the effect of $F\mathfrak{C}_{fz}$ by comparing *Hint*-$F\mathfrak{C}_{fz}$ and *Hint*.

Exp3. To compare the proposed *Hint*-$F\mathfrak{C}_{fz}$ with Ch_{03}-$F\mathfrak{C}_{fz}$, with both following the direct approach.

Exp4. To compare *Hint*-$F\mathfrak{C}_{fz}$ with four indirect methods, namely ESIHE [64], RICE [65], GHMF [66], and ROHIM [67].

If these experiment results could provide affirmative answers, we might conclude that the above proposed components actually have practical meaning.

5.1. Experiment preparation

First, we need a preparation including a proposal of new luminance homogeneity measurement of image region, which can contribute to improve the contrast measure operator $\mathcal{C}_{\mathbb{c},b}$, and a discussion of criteria of quality assessment of multichannel images.

5.1.1. Proposal for a new local homogeneity measurement

The main contribution of the study [21] is its proposed local homogeneity measurement of the luminance values of a window w_{ij} of the image pixel p_{ij}, denoted by $HO_{Ch03}(l_{ij}, w_{ij})$, which are in turn defined by its opposite notion, the measure of local non-homogeneity of this window, and an image contrast measure of the pixel. Because that study shows the significant role of homogeneity measurement, it is necessary to examine it more carefully to define it.

The homogeneity measurement $HO_{Ch03}(l_{ij}, w_{ij})$ within a window w_{ij} is defined as a function of four factors: the edge value describing the magnitude of the gradient at p_{ij}; the standard deviation, which is the luminance dispersion within w_{ij} around l_{ij}; the entropy, which is the distribution variation; and γ_4, which is the impulsiveness of the distribution in w_{ij}. These values, which are normalised in [0, 1], and their complements representing the negation of the respective factors, are calculated and denoted respectively by $\overline{E(l_{ij}, w_{ij})}$, $\overline{V(l_{ij}, w_{ij})}$, $\overline{H(l_{ij}, w_{ij})}$, and $\overline{R_4(l_{ij}, w_{ij})}$. Then, we have [21]

$$HO_{Ch03}(l_{ij}, w_{ij}) = \overline{E(l_{ij}, w_{ij})} * \overline{V(l_{ij}, w_{ij})} * \overline{H(l_{ij}, w_{ij})} * \overline{R_4(l_{ij}, w_{ij})} \quad (26)$$

However, by analysing our performed experiments, we observe that by applying such HO_{Ch03}, the quality of the images is not always good. For example, the image in Fig. 5a pixelwise exposed by the HO_{Ch03} values of the image I04 is clearly not smooth by human visual perception. Maybe this is because these factors play an equal role in such a combination. To seek for a better aggregation of these factors, we examined more than 30 combinations using various operators such as min, max, product, Yager, Zimmerman, Hamacher, Dombi, Aczel, and weighted average, which can be found in [68]. We observe that while the two factors $\overline{V(l_{ij}, w_{ij})}$ and $\overline{R_4(l_{ij}, w_{ij})}$ are continuous, the two remaining ones are not. This suggests us to introduce the following aggregation Max-Product (*MP*), for our combination:

$$HO_{MP}(l_{ij}, w_{ij}) = \max\left\{\overline{E(l_{ij}, w_{ij})} * \overline{H(l_{ij}, w_{ij})}, \overline{V(l_{ij}, w_{ij})} * \overline{R_4(l_{ij}, w_{ij})}\right\} \quad (27)$$

To demonstrate the effect of this *HO*-measure HO_{MP}, we expose two images given in Fig. 5a and 5c pixelwise representing the local homogeneity values of image I04 computed, respectively, by the *HO*-measure HO_{Ch03} defined in (26) and by HO_{MP} defined in (27) for comparison. They show that Fig. 5c is much smoother and much brighter than Fig. 5a. Similarly, the output image made by the method Ch_{03} itself but using the local values computed

Fig. 4. Some selected original different low contrast images for experiments: three dark images #1 to #3 and three bright images I03, I04, and I07.

Fig. 5. (a) Image formed by the homogeneity of RGB-image I04 using HO_{Ch03} (b) Output image of method Ch_{03} using HO_{Ch03} (c) Image formed by the homogeneity of RGB-image I04 using HO_{MP} (d) Output image of method Ch_{03} using HO_{MP}.

based on HO_{MP} instead of its HO_{Ch03}, shown in Fig. 5d, is smoother than the output image of the same method but using those values calculated based on its own original HO_{Ch03} given in Fig. 5b, in which the rectangle-marked regions are not quite smooth and have lost certain details. Hence, from now on, the HO_{MP} in (27) will always be used instead of HO_{Ch03} for *Hint*.

5.1.2. Criteria for image quality assessment

To analyse and assess the experiment results, human visual criterion, an objective criterion for direct image contrast assessments, and some other objective criteria for indirect image contrast assessments are taken into consideration. Due to the complexity of image quality assessment, none of them is the best and they complement each other in assessing the quality of the images obtained. They comprise the following:

(1) *Contrast measure criterion CM*. We consider the following objective criterion, which is the mean of the image contrast measurement defined in (28), in which $b = \delta_k(i, j)$ is the mean non-homogeneity grey value at pixel p_{ij} of the k channel defined in [21] but using HO_{MP} defined by (27) instead of HO_{Ch03}.

$$CM_\delta\ (\mathrm{i}_k) = \sum_{i,j} \frac{|\mathrm{i}_k(i,j)-\delta_{\mathrm{i}_k}(i,j)|}{\mathrm{i}_k(i,j)+\delta_{\mathrm{i}_k}(i,j)} / MN \tag{28}$$

(2) *Entropy criterion $E_{avg}(\mathrm{i})$*. It is known that the entropy and fuzzy entropy indicators examined for the objective criterion can reveal finer details that do not clearly appear in the original image. The entropy of an image indicates the average information of the whole image and the higher the entropy, the richer the details of the raw image that the contrast-enhanced image can preserve. Therefore, similarly as above, we introduce the following objective criterion:

$$E_{avg}\ (\mathrm{i}) = \frac{\sum_{k=1}^{K} E(\mathrm{i}_k)}{K} \tag{29}$$

where $E\ (\mathrm{i}_k) = -\sum_{l_k=L_{k,min}}^{L_{k,max}} p_k(l_k) \log_2(p_k\ (l_k))$, for $p_k\ (l_k) = \frac{\mathfrak{h}_k(l_k)}{MN}$

(3) *Fuzzy entropy criterion E_{linF}*. For every fuzzificator F of a k-channel image i_k of i with its fuzzy membership function μ_F, the fuzzy entropy of i_k, denoted by E_F, is defined as given in Box I:

Let F be a natural transformation, $\mu_{linF}\ (\mathrm{i}_k\ (i, j)) = \tilde{\mathrm{i}}_k(i, j) = \frac{l_k(i,j)-L_{k,min}}{L_{k,max}-L_{k,min}}$. Then,

$$E_{linF}(\mathrm{i}_k) = -\frac{\sum_{i,j}\left(\tilde{\mathrm{i}}_k(i,j)\log_2\left(\tilde{\mathrm{i}}_k(i,j)\right) + \left(1-\tilde{\mathrm{i}}_k(i,j)\right)\log_2\left(1-\tilde{\mathrm{i}}_k(i,j)\right)\right)}{MN},$$

and put

$$E_{linF,avg}(\mathrm{i}) = \frac{\sum_{k=1}^{K} E_{linF}(\mathrm{i}_k)}{K} \tag{30}$$

The fuzzy entropy of a fuzzification of an image can be considered as a useful criterion of image quality. The lower the fuzzy entropy, the higher the contrast of the whole image.

5.2. Experiments and comparative analysis

We subsequently perform the four aforementioned experiments Exp1 to Exp4. In the comparative study, the quantitative criteria presented above will be applied to assess the quality of the input images as well as the respective output images of both methods in each experiment. By their objectives, Exp1 and 2 are

$$E_F(\mathrm{i}_k) = -\frac{\sum_{i,j} (\mu_F(\mathrm{i}_k\,(i,j)) \log_2 (\mu_F\,(\mathrm{i}_k\,(i,j))) + (1-\mu_F\,(\mathrm{i}_k\,(i,j))) \log_2 (1-\mu_F\,(\mathrm{i}_k\,(i,j))))}{MN}.$$

Box I.

Table 4
Determined parameter values of *Hint* $\mathfrak{C}_{fz}$.

For $\mathcal{AX}_{k,ij}$	For $\mathcal{AY}_{k,ij}$
$fm_{\mathcal{X}_{k,ij}}(c^-) = \delta_{k,ij}(F_k(\mathrm{i}_k))$	$fm_{\mathcal{Y}_{k,ij}}(c^-) = fm_{\mathcal{X}_{k,ij}}(c^-)$
$\beta_{\mathcal{X}_{k,ij}} = 0.6$	$\beta_{\mathcal{Y}_{k,ij}} = \sqrt{\xi_{k,ij}\beta_{\mathcal{X}_{k,ij}}}$

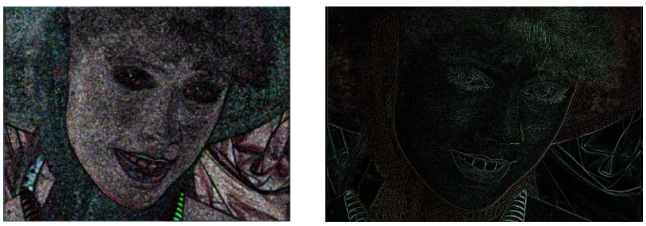

(a) (b)

Fig. 6. Difference of the output of *Ch*03 applied to image I04 and its original: (a) Image formed by the homogeneity of the RGB-image I04 using HO_{Ch03} (b) Difference of the output image luminance and its original multiplied by 10.

performed on RGB images, whereas Exp3 and 4 are performed on both RGB and HSV images. For the operator *Hint*, depending on the requirement of each experiment, the luminance surrounding value at each pixel is computed using either the proposed HO_{MP} or HO_{Che03}. The values of the fuzziness parameters of *Hint* are determined as given in Table 4 and used for all experiments.

Exp1: *Hint* vs. Ch_{03}. To show the actual performance of the component *Hint*, before it is integrated into *Hint-F*$\mathfrak{C}_{fz}$ as a whole, it is necessary to compare *Hint* with the method Ch_{03} examined in [21]. That is, *Hint* and Ch_{03} are applied to the same image fuzzified by the 'natural' fuzzificator, which in nature is the normalisation of the luminance domain $[L_{min}, L_{max}]$ into [0, 1]. In addition, the local features $\delta_{k,ij}$ and $\xi_{k,ij}$ commonly used for both *Hint* and Ch_{03} must be equal and the related parameters to run both operators must also be the same. Here, the experiment is organised to be able to compare the effectiveness of both operators on each channel, *R*, *G*, and *B*, as well as on the entire RGB image itself. Under such conditions, we can properly assess their effectiveness using the objective criteria discussed above.

To execute the experiment, the only common running parameter *d* indicating the window size of each pixel is set as $d = 3$ for both operators to guarantee that all the common local image feature values are equal. The only one running parameter of Ch_{03}, which is the exponent *t* of the amplification constant $\xi_{k,ij}$, is set as $0.25 \in \{0.25, 0.5\}$. Moreover, except for the parameter values given in Table 4, the fuzziness parameter $\alpha_{k,ij} = \mu(Little)$ of *Hint* is set as 0.4.

The experiment results produced by *Hint* and Ch_{03} acting on the six input images given in Fig. 4 and assessed by the criterion *CM* applied to each individual channels *R*, *G*, and *B* of their output images and by the entropy criteria E_{avg} and $E_{linF,avg}$ applied to the whole output images are presented in Table 5. It shows that *Hint* is better than Ch_{03} in almost cases and this demonstrates generally that the performance of *Hint* is more effective than that of Ch_{03}, noting that in contrast to E_{avg}, for E_{linF}, the larger the value of E_{linF}, the lower the contrast feature of the whole image.

To assess the performance of *Hint* and Ch_{03} in relation to HO_{Ch03} with respect to the human visual perception, we apply both operators to, for instance, image I04, which has a low contrast. Fig. 6a shows the image representing simultaneously the homogeneity values $HO_{Ch03,ij}$'s of all three individual channel images of image I04 and Fig. 6b represents the difference of the luminance of Ch_{03}'s output image i' of image I04 with the luminance range [0, 255] and the luminance of its original one after multiplying by 10 for an acceptable human visual perception. By a rule discussed in [21], the image shown in Fig. 6a shows that the brighter (darker) the degree of its region, the higher (lower) the homogeneity of the corresponding region of the original image, which implies smaller (larger) contrast changes made by the ICE method in this region of the original image. It can easily be observed by human visual perception that it is very difficult to observe the luminance variation of the image given in Fig. 6b, and even in very dark regions such as those around the eyes of the image, the luminance variations on these regions are very small. The homogeneity measure on the regions of the input image corresponding to these dark luminance regions of Fig. 6a are low, on which it is required to enhance their contrast more, according to the rule in [21] just mentioned. The method Ch_{03} to enhance the image contrast by applying a power transformation with its base smaller than 1 and its exponent being the amplification constant $\xi_{k,ij}$ [21] is developed by utilising the above rule: the larger the $\xi_{k,ij}$ value, which is equivalent to a higher homogeneity on an image region, the smaller the degree of contrast enhancement made by Ch_{03} on this region. However, Fig. 6b shows that the degree of contrast enhancement of image I04 made by Ch_{03} is still small. Although *Hint* can change the image contrast at each pixel better, the same situation still occurs in our experimental study of *Hint*. This shows that the functionality of HO_{Ch03} is not as expected.

∘ *Exp2*: *Hint-F*$\mathfrak{C}_{fz}$ vs. *Hint* to show the expected functionality of $F\mathfrak{C}_{fz}$. As discussed in the end of Section 4, for the proposed method *Hint-F*$\mathfrak{C}_{fz}$, the clustering operator $F\mathfrak{C}_{fz}$ acts on the whole image $\mathrm{i} = (\mathrm{i}_R, \mathrm{i}_G, \mathrm{i}_B)$ to cluster it into *C* clusters. Then, for every cluster c, $c = 1$ to *C*, the dynamic ranges of grey levels of i_k, $B_{ck1}(f)$ and $B_{ck2}(f)$, are computed, where *f* is a constant parameter and $k \in \{R, G, B\}$. Based on these values, the fuzzificator F_k of the channel image i_k is established by the formula given in Point 1.4 of Step 1 of the method *Hint-F*$\mathfrak{C}_{fz}$ in Section 4.3, which may be considered as an 'average aggregation' of *C* natural fuzzificators of the dynamic ranges of the individual clusters *c*'s, $c = 1$ to *C*. In running $F\mathfrak{C}_{fz}$, *C* (in {2, …, 10}) is set as 5 and $f = 0.005$. Formally, there is a significant difference between $F\mathfrak{C}_{fz}$ and the fuzzificator examined in [22], denoted by F_{Ch0}, as follows: whereas, for each channel, the operator F_{Ch0} seeks for only a unique dynamic range of grey levels in the whole domain [0, 255], $F\mathfrak{C}_{fz}$ tries to seek for *C* dynamic ranges, where *C* is the number of clusters. In addition, it should deal with all image channels in relation to each other by running on the total input image.

As argued previously, in this experiment, both operators *Hint-F*$\mathfrak{C}_{fz}$ and *Hint* are applied to six raw images given in Fig. 4. The experiment results are assessed by the aforementioned criteria and listed in Table 6, in which the best criteria values are in bold. It shows that the operator *Hint-F*$\mathfrak{C}_{fz}$ produces better output images than *Hint* does for all 6 raw images assessed by criteria CM_G, CM_B, and E_{avg}. It performs better than *Hint* for all 6 raw images except

Table 5
Comparison of contrast intensification of Ch_{03} and *Hint* applied on six given original RGB images with respect to criterion *CM* on each channel and to E_{avg} and $E_{linF,avg}$, where the bold figures indicate the better values of the respective criteria.

Criteria	*CM*									E_{avg}			$E_{linF,avg}$		
Image	*R*			*G*			*B*								
	Origin.	Ch_{03}	*Hint*	Origin.	Ch_{03}	*Hint*	Origin.	Ch_{03}	*Hint*	Origin.	Ch_{03}	*Hint*	Origin.	Ch_{03}	*Hint*
#1	0.1180	0.1241	**0.1540**	0.1914	0.1981	**0.2325**	0.2482	0.2538	**0.2859**	5.9395	**6.0291**	5.9565	0.3456	0.3509	**0.3424**
#2	0.0160	0.0168	**0.0203**	0.0191	0.0205	**0.0272**	0.0314	0.0349	**0.0563**	7.3150	7.3186	**7.3423**	0.8216	**0.8214**	0.8219
#3	0.0273	0.0299	**0.0391**	0.0304	0.0330	**0.0429**	0.0364	0.0395	**0.0517**	3.4443	3.5617	**3.7168**	0.2861	0.2850	**0.2825**
I03	0.0154	0.0169	**0.0228**	0.0188	0.0202	**0.0264**	0.0548	0.0569	**0.0689**	7.4847	7.4849	**7.4945**	0.8001	0.8001	**0.7986**
I04	0.0170	0.0178	**0.0216**	0.0293	0.0307	**0.0380**	0.0345	0.0359	**0.0433**	7.3092	7.3033	**7.3195**	0.8504	0.8521	**0.8496**
I07	0.0256	0.0273	**0.0350**	0.0298	0.0324	**0.0443**	0.0511	0.0537	**0.0664**	7.4536	7.4561	**7.4763**	0.8642	0.8639	**0.8613**

image #3 based on CM_R but it performs better only on 2 raw images #1 and #3, based on criterion $E_{linF,avg}$.

It is necessary to note that these objective criteria are global characteristics because, by their definitions ((29) and (30)), they are arithmetic averages of image contrast quantities pixelwise defined. These characteristics indicate the degrees of contrast changes that the corresponding image *CI*s can make in the total image, but it cannot guarantee the quality of the improved local image details. Therefore, the human visual perception is still very crucial to evaluate the quality of the output images. However, in the global viewpoint, these experiment results still show the expected functionality of the fuzzy clustering $F\mathfrak{C}_{fz}$.

∘ *Exp3*: *Hint*-$F\mathfrak{C}_{fz}$ vs. Ch_{03}-$F\mathfrak{C}_{fz}$. First, it should be noted that in order to obtain an accurate conclusion, in this comparative study, we use Ch_{03}-$F\mathfrak{C}_{fz}$ instead of Ch_{03} as the fuzzificator of Ch_{03} examined in [21], which in nature is only the normalisation of $[L_{\min}, L_{\max}]$ to the interval [0, 1]. When the experiment could show the better performance of the proposed method *Hint*-$F\mathfrak{C}_{fz}$, we may conclude that *Hint*-$F\mathfrak{C}_{fz}$ would be actually better than Ch_{03}, even when the latter uses also the better measurement HO_{MP} instead of HO_{Ch03} and is augmented by the FCM $F\mathfrak{C}_{fz}$. To perform Exp3, the values of the running parameters of the operators *Hint*, $F\mathfrak{C}_{fz}$, and Ch_{03} are set the same as those in Exp2. The image data consist of 27 raw images with 24 images of TID2013 and three selected ones (#1 to #3), which are either of high darkness or of low contrast, as aforementioned. Both RGB and HSV representations of the image are all under consideration. Similar to the above, the experiment results are also assessed by the objective criteria and the relative percentage difference of each criterion value of an output image produced by *Hint*-$F\mathfrak{C}_{fz}$ and the respective one produced by Ch_{03}-$F\mathfrak{C}_{fz}$ are listed in Table 7, in which the better criteria values are in bold. It shows that the percentage of the better criteria values of *Hint*-$F\mathfrak{C}_{fz}$ vs. Ch_{03}-$F\mathfrak{C}_{fz}$ are approximately as follows: 96% for the first three columns, 100% for the next three columns, 85% for the 7th column, 89% for both the 8th column and the last column, and 67% for the 9th column. These strongly demonstrate that *Hint*-$F\mathfrak{C}_{fz}$ actually outperforms the counterpart operator with respect to these global criteria.

∘ *Exp4*: *Hint*-$F\mathfrak{C}_{fz}$ vs. *enhancement intensificators of indirect methods*. To simplify the presentation and space, in this experiment, we analyse the experiment results using only the criteria E_{avg} and $E_{linF,avg}$, which are related to the global and local feature details and the human visual perception when we expose the images in question in HSV format. As aforementioned, although an image contrast intensification method may be evaluated to be better than another one by these objective criteria, it may still cause losses of necessary image details. Thus, the human visual perception is still necessarily applied to evaluate its effectiveness.

Four contrast intensification methods of the indirect approach, namely ESIHE [64], RICE [65], GHMF [66], and ROHIM [67], are considered as the counterpart *CI*s, whose algorithms described in those papers can also be found in [64,69]. The raw image data and the run parameters of our proposed method are the same as above. The criteria values of the output images of the *CI*s under consideration represented in HSV format are given in Table 8, in which the best values are in bold. It is observed that 17/27 (63%) best E_{avg} values of the output images are produced by *Hint*-$F\mathfrak{C}_{fz}$, but only 2/27 (7%) best $E_{linF,avg}$ values are attributable to *Hint*-$F\mathfrak{C}_{fz}$.

However, by the human visual perception, we show that the counterpart methods with better values of E_{avg} or $E_{linF,avg}$ may cause more losses in local image details than *Hint*-$F\mathfrak{C}_{fz}$. In fact, because most $E_{linF,avg}$ values of the output images produced by GHMF given in Table 8 are the best, this suggests first to compare the performance of GHMF and *Hint*-$F\mathfrak{C}_{fz}$. Let us examine the difference of the corresponding $E_{linF,avg}$ values of the output images of the two methods given in the column 'GHMF *Hint*-$F\mathfrak{C}_{fz}$'. Owing to the limitation of presentation space, we show the output images of three input images selected to ensure diversity of the comparison. The remaining output images of the methods can be found in [70]. First, we consider two images I02 and I24, which attain respectively the largest difference value, −0.22, and the median value −0.0836 of the range [−0.22, 0.0468] of the values of column 'GHMF \ *Hint*-$F\mathfrak{C}_{fz}$'. Second, we also consider image I10 because it has the smallest $E_{linF,avg}$ value of its output image of ROHIM examined in [67], which was recently published in 2017. In addition, it can be checked that, for this image, the difference of the $E_{linF,avg}$ values of its output images of methods *Hint*-$F\mathfrak{C}_{fz}$ and ROHIM is −0.1217, which also is approximately a median value in between the minimum and maximum difference values of −0.2165 and 0.0051, respectively. In addition, the $E_{linF,avg}$ values of 0.5130, 0.7264, and 0.7065, respectively, of the output images of I02 and I24 produced by operator GHMF and of the output image of I10 produced by ROHIM are the best among the $E_{linF,avg}$ values of the five operators considered. The raw images I02, I10, and I24 and their respective output images produced by all these operators are exhibited, respectively, in Figs. 7–9. However, by the human visual perception, it can be observed in general that the colours of their output images produced by *Hint*-$F\mathfrak{C}_{fz}$ given respectively in Figs. 7f–9f seem to be more natural and their details become more visible than the remaining output images, which show that many details are more clearly revealed by *Hint*-$F\mathfrak{C}_{fz}$. For illustration, it can be observed that the selected marked regions of the raw images as well as of their respective output images of *Hint*-$F\mathfrak{C}_{fz}$ shown in Figs. 7–9 in general are perceived more colourfully and clearly than the respective ones produced by the counterpart methods. Furthermore, many details in these regions are more clearly visualised.

Particularly, focusing on the marked regions of the images in Fig. 7, in which the raw image is dark and of low contrast, it can also be observed that the proposed method is actually able to preserve global features as well as local details of the raw image. This shows that *Hint*-$F\mathfrak{C}_{fz}$, as a direct method, can achieve a reasonable balance between global features and local ones when changing the image contrast.

Table 6
Comparison between the performance of *Hint*-$F\mathfrak{C}_{fz}$ and *Hint* with respect to the criteria in question, where bold numbers indicate the best values and italic numbers the worst values.

Image	CM_R		CM_G		CM_B		E_{avg}		$E_{linF,avg}$	
	Hint-$F\mathfrak{C}_{fz}$	*Hint*	*Hint*-$F\mathfrak{C}_{fz}$	*Hint*	*Hint*-$F\mathfrak{C}_{fz}$	*Hint*	*Hint*-$F\mathfrak{C}_{fz}$	*Hint*	*Hint*-$F\mathfrak{C}_{fz}$	*Hint*
#1	**0.3067**	0.1540	**0.4422**	0.2325	**0.5537**	0.2859	**6.7621**	*5.9565*	*0.4966*	**0.3424**
#2	**0.0503**	0.0203	**0.0982**	0.0272	**0.0579**	0.0563	**7.3506**	7.3423	**0.7707**	*0.8219*
#3	0.0373	**0.0391**	**0.0441**	0.0429	**0.0548**	0.0517	**3.7398**	3.7168	*0.2923*	**0.2825**
I03	**0.0602**	0.0228	**0.0988**	0.0264	**0.1491**	0.0689	**7.6852**	7.4945	**0.7935**	0.7986
I04	**0.0909**	0.0216	**0.1741**	0.0380	**0.1973**	0.0433	**7.6426**	7.3195	**0.8419**	0.8496
I07	**0.1002**	0.0350	**0.1464**	0.0443	**0.1876**	0.0664	**7.8066**	7.4763	**0.7929**	0.8613

Table 7
Contrast enhancement degree of *Hint*-$F\mathfrak{C}_{fz}$ (%) compared to Ch_{03}-$F\mathfrak{C}_{fz}$ when they are applied to RGB format and HSV format of 27 given raw images.

Image	*CM*						E_{avg}		$E_{linF,avg}$	
	R		*G*		*B*					
	RGB	HSV	RGB	HSV	RGB	HSV	RGB	HSV	RGB	HSV
#1	**09.38**	**144.24**	**06.02**	**072.19**	**04.14**	**062.04**	**2.27**	**12.23**	*2.410*	*34.13*
#2	**05.23**	**444.51**	**03.59**	**023.92**	**05.66**	**237.96**	*−0.31*	**1.56**	*0.360*	**−08.91**
#3	*05.97*	**185.63**	*−06.57*	**163.06**	**12.30**	**142.50**	**1.20**	**9.96**	*1.460*	*15.17*
I01	**12.36**	**175.65**	**04.98**	**173.21**	**09.08**	**185.46**	*−0.35*	**7.68**	**−0.340**	**−16.13**
I02	**11.70**	**304.68**	**03.89**	**198.28**	**02.99**	**118.42**	**4.95**	**7.24**	*0.050*	*01.36*
I03	**05.24**	**352.98**	**02.70**	**243.28**	**07.81**	**062.99**	**0.34**	**1.53**	**−0.001**	**−04.39**
I04	**02.48**	**457.80**	**03.88**	**425.58**	**05.00**	**491.01**	*−0.01*	**5.93**	*0.110*	**−09.16**
I05	**11.71**	**101.72**	**08.36**	**102.86**	**10.09**	**072.35**	**0.78**	**0.89**	*0.000*	**−07.88**
I06	**01.67**	**198.47**	**01.37**	**159.40**	**12.16**	**115.31**	**0.45**	**1.58**	**−0.610**	**−09.12**
I07	**03.62**	**116.22**	**05.02**	**092.22**	**05.16**	**108.18**	**0.16**	**2.28**	**−0.340**	**−03.89**
I08	**17.42**	**111.34**	**01.34**	**114.43**	**08.58**	**171.62**	**0.25**	−0.03	**−1.100**	**−09.81**
I09	**03.91**	**274.68**	**07.47**	**353.12**	**04.55**	**479.77**	**0.51**	**3.63**	**−0.670**	**−11.28**
I10	**08.97**	**438.25**	**08.66**	**432.32**	**07.87**	**806.81**	**0.62**	**4.61**	**−0.980**	**−08.05**
I11	**05.16**	**088.11**	**04.40**	**064.89**	**06.26**	**55.12**	**0.42**	**2.19**	**−0.170**	**−06.96**
I12	**09.05**	**365.97**	**07.43**	**609.36**	**09.92**	**400.39**	**0.71**	**3.68**	**−0.290**	**−05.83**
I13	**18.81**	**015.48**	**15.23**	**009.61**	**13.65**	**008.90**	**0.90**	**1.60**	**−1.650**	**−11.27**
I14	**02.54**	**232.72**	**08.37**	**220.46**	**05.77**	**141.94**	**0.32**	**0.56**	**−0.360**	**−07.07**
I15	**05.81**	**238.98**	**07.29**	**113.66**	**05.63**	**249.31**	**1.62**	**2.53**	*0.180*	**−07.31**
I16	**07.75**	**248.07**	**07.60**	**272.16**	**09.37**	**376.76**	**1.04**	**5.59**	**−1.010**	**−07.84**
I17	**03.73**	**244.41**	**04.94**	**194.51**	**04.97**	**227.00**	**0.90**	**4.26**	*0.080*	**−08.00**
I18	**11.00**	**148.29**	**09.46**	**119.31**	**06.63**	**088.34**	**1.41**	**2.11**	*0.120*	**−04.16**
I19	**02.45**	**051.31**	**05.31**	**094.55**	**13.92**	**079.52**	**0.55**	**0.77**	**−0.630**	**−05.21**
I20	**10.32**	**360.89**	**04.92**	**365.57**	**00.71**	**402.51**	*−0.00*	*−2.32*	**−0.130**	**−01.82**
I21	**84.39**	**253.75**	**37.57**	**245.56**	**62.67**	**257.56**	**2.50**	**2.29**	**−9.760**	**−08.42**
I22	**07.99**	**198.12**	**04.73**	**240.05**	**05.40**	**274.03**	**0.16**	**0.37**	**−0.770**	**−16.00**
I23	**01.58**	**768.02**	**07.18**	**775.61**	**09.53**	**400.49**	**0.37**	*−0.57*	**−0.180**	**−10.15**
I24	**08.97**	*100.52*	**06.18**	**140.23**	**06.27**	**280.08**	**1.00**	**5.07**	**−0.630**	**−08.16**
Mean	**10.341**	**245.215**	**6.716**	**222.941**	**9.485**	**233.199**	**0.843**	**3.230**	**−0.550**	**−5.413**

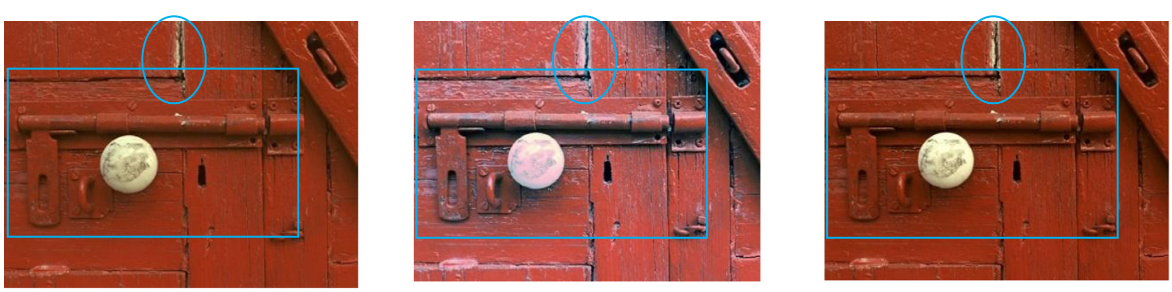

(a) Original image I02 (b) ESIHE [ID1] $E_{linF,a}$ = 0.8248 (c) RICE [ID4] $E_{linF,avg}$ = 0.6791

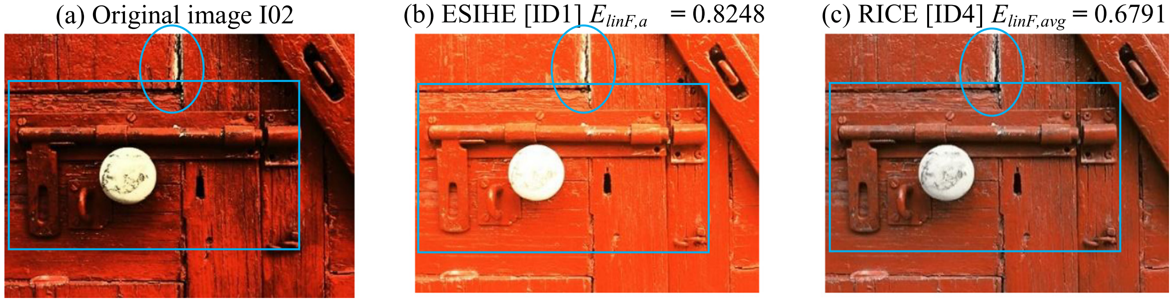

(d) GHMF [ID3] $E_{linF,avg}$ = **0.5130** (e) ROHIM [ID2] $E_{linF,avg}$ = 0.5165 (f) *Hint*-$F\mathfrak{C}_{fz}$ $E_{linF,avg}$ = 0.7330

Fig. 7. Output images of raw image I02 of image database TID2013 produced by operators under consideration for human visual perception.

Table 8
Values of criteria $\boldsymbol{E_{avg}}$ and $\boldsymbol{E_{LinF,avg}}$ of output images of enhanced intensificators under consideration, whose raw images are presented in HSV format, where the best values are in bold.

Image ID	Raw images	E_{avg}					$E_{LinF,avg}$					
		ESIHE	RICE	GHMF	ROHIM	*Hint-F*$\mathfrak{C}_{fz}$	ESIHE	RICE	GHMF	ROHIM	*Hint-F*$\mathfrak{C}_{fz}$	GHMF \ *Hint-F*$\mathfrak{C}_{fz}$
#1	5.9395	6.6176	5.1207	**6.7002**	5.3846	6.6628	0.5211	**0.2793**	0.4523	0.6478	0.4574	−0.0051
#2	7.3154	7.4691	7.4358	7.1781	6.8435	**7.4364**	0.7946	0.7659	0.7019	**0.5866**	0.7479	−0.0460
#6	3.4443	3.4886	3.6743	3.2663	3.4442	**4.1248**	0.2632	0.2240	**0.1636**	0.3339	0.3288	−0.1652
I01	7.2409	7.5023	7.4543	7.6470	7.2075	**7.8945**	0.8007	0.8502	**0.7129**	0.8529	0.7453	−0.0324
I02	7.0231	6.9740	7.1843	6.7369	6.2869	**7.5610**	0.8248	0.6791	**0.5130**	0.5165	0.7330	**−0.2200**
I03	7.4847	7.4876	7.4834	7.2844	6.8306	**7.6009**	0.7554	0.7444	0.7042	**0.5790**	0.7643	−0.0601
I04	7.3092	7.4382	7.5612	7.1560	6.8622	**7.7425**	0.7876	0.8091	0.7627	**0.5902**	0.7734	−0.0107
I05	7.5728	7.6214	7.5884	7.2797	7.1495	**7.6645**	0.7343	0.6616	**0.6163**	0.6613	0.6707	−0.0544
I06	7.6130	7.7328	7.6934	7.4857	7.4825	**7.7575**	0.7258	0.7621	0.7238	**0.7187**	0.7286	−0.0048
I07	7.4536	7.5746	7.5646	7.3305	7.2661	**7.6393**	0.8095	0.8124	**0.7817**	0.7439	0.8285	−0.0468
I08	7.6508	7.7452	7.6566	7.4656	7.3609	**7.6859**	0.7252	0.7236	**0.6881**	0.7051	0.6980	−0.0099
I09	7.4954	7.6984	7.6397	7.4251	7.4188	**7.7932**	0.7597	0.8545	0.8034	0.8079	0.7843	0.0191
I10	7.3664	7.6917	7.5409	7.8570	7.1014	**7.7312**	0.7941	0.8718	0.7167	**0.7065**	0.8282	−0.1115
I11	7.3929	7.5068	7.4247	7.1441	7.2649	**7.5803**	0.7489	0.7069	**0.6685**	0.8193	0.7130	−0.0445
I12	7.4530	7.5553	7.5594	7.3350	7.2926	**7.7387**	0.7690	0.7879	**0.7145**	0.7896	0.7732	−0.0587
I13	7.5329	7.6081	7.6283	7.3750	7.3116	**7.6849**	0.7528	0.7501	0.7081	0.7788	**0.7076**	0.0005
I14	7.6961	7.7429	**7.7889**	7.5014	7.3843	7.7615	0.7521	0.7566	0.7024	**0.6611**	0.7468	−0.0444
I15	7.1638	7.3422	7.0858	6.7842	6.7314	**7.3635**	0.7224	0.5729	**0.5075**	0.7503	0.5981	−0.0906
I16	7.2633	7.5921	7.4561	**7.8294**	7.1905	7.6884	0.8147	0.8800	**0.7290**	0.8702	0.8417	−0.1127
I17	7.3354	7.3672	7.4038	**7.7182**	7.2719	7.6628	0.7002	0.6666	**0.6439**	0.7852	0.6816	−0.0377
I18	7.1717	7.4235	7.2446	6.8988	7.0403	**7.3641**	0.7904	0.6570	**0.5954**	0.8565	0.7002	−0.1048
I19	7.7222	7.8068	**7.7969**	7.5689	7.5784	7.7948	0.7692	0.7851	**0.7580**	0.7624	0.7860	−0.0280
I20	**6.3135**	6.3247	6.1416	5.7374	6.2451	6.2145	0.4733	0.4089	**0.3367**	0.4544	0.4429	−0.1062
I21	7.3067	**7.5464**	7.4677	7.2190	7.2245	7.5102	**0.7913**	0.8416	0.8111	0.8177	0.7996	0.0115
I22	7.4309	**7.6705**	7.6164	7.3454	7.3408	7.4774	0.7343	0.8006	0.7598	0.7919	**0.7130**	0.0468
I23	7.7178	7.7288	**7.7859**	7.5482	7.5328	7.6828	0.7451	0.7528	**0.6995**	0.7170	0.7194	−0.0199
I24	7.0790	7.3761	7.3259	**7.7730**	7.0280	7.4819	0.7726	0.8358	**0.7264**	0.8808	0.8100	−0.0836

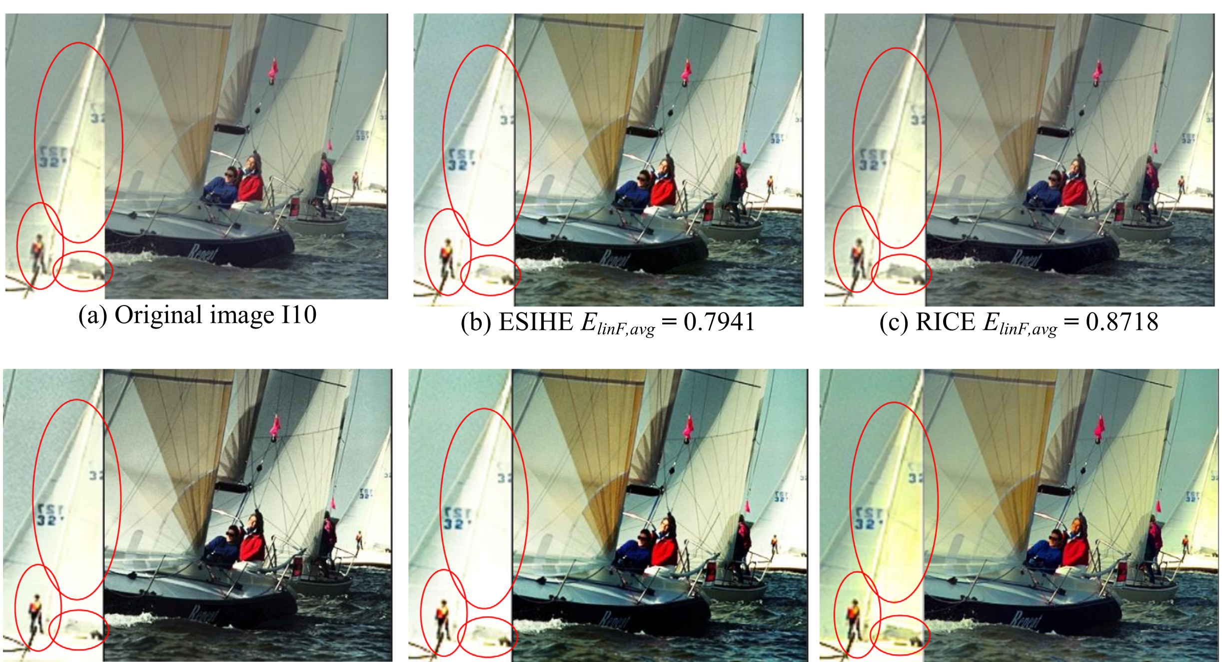

(a) Original image I10 (b) ESIHE $E_{linF,avg} = 0.7941$ (c) RICE $E_{linF,avg} = 0.8718$
(d) GHMF $E_{linF,avg} = 0.7167$ (e) ROHIM $E_{linF,avg} = \mathbf{0.7065}$ (f) *Hint-F*$\mathfrak{C}_{fz}$ $E_{linF,avg} = 0.8282$

Fig. 8. Output images of raw image I10 of image database TID2013 produced by operators under consideration for human visual perception.

6. Conclusions and future study

ICE is one of the most important issues of image processing, pattern recognition, and computer vision, and it attracts much attention from researchers in this field. However, most recent studies rely upon indirect methods that deal with the image histogram, whose values are grey level frequencies of images. The direct methods changing the luminance at each pixel are more effective than the indirect ones [21], but only few studies follow them. For the latter methods, it is crucial that such changes of luminance at the individual image pixels can be considered as a luminance function, which, based on expert experience, should be in the form of an S function. As these changes mostly affect local features on a given image, it is required that they are realised in a 'combined manner' in order to maintain the global information of the entire image. Thus, the direct approach seems to be more

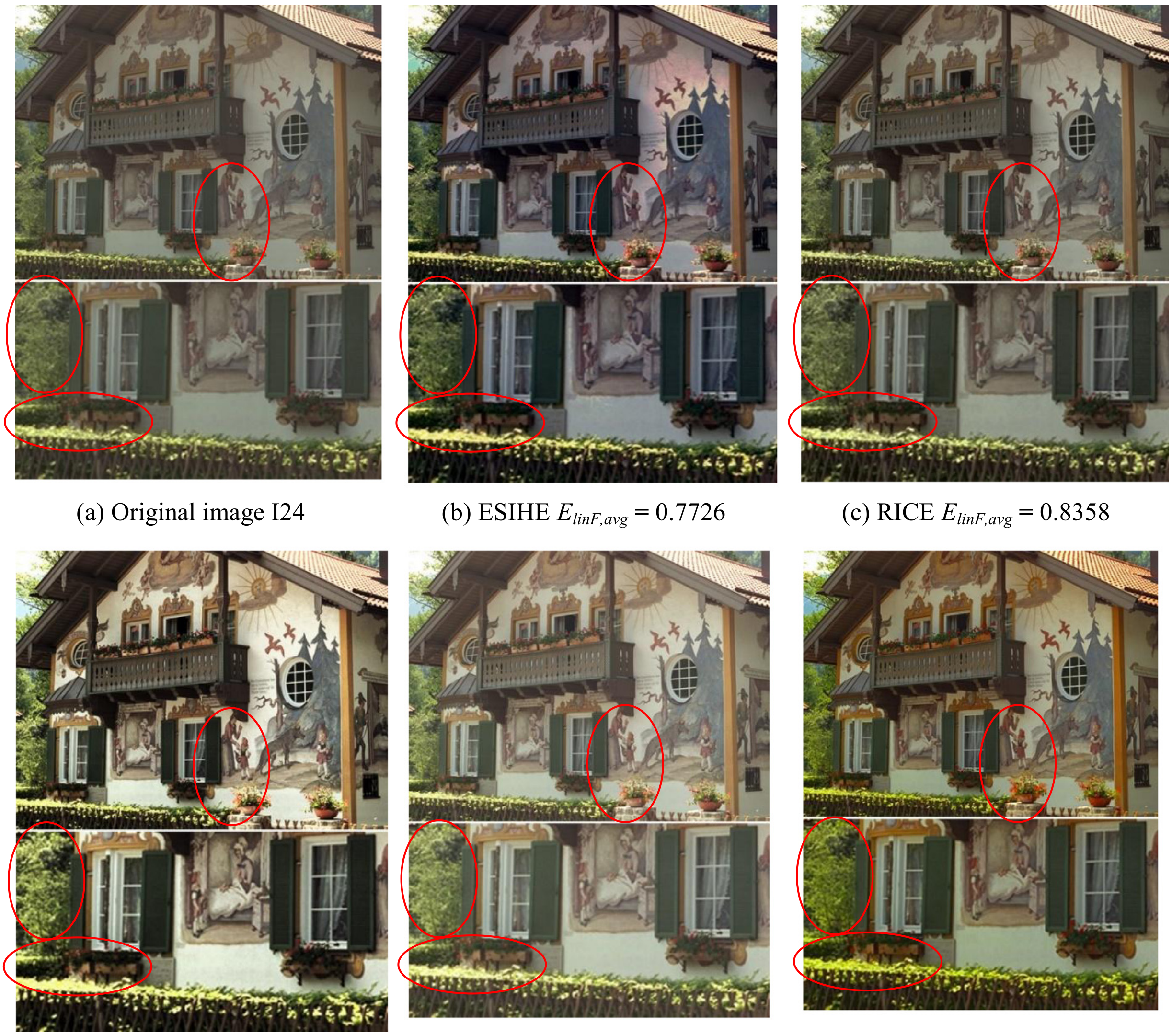

(a) Original image I24 (b) ESIHE $E_{linF,avg} = 0.7726$ (c) RICE $E_{linF,avg} = 0.8358$

(d) GHMF $E_{linF,avg} = \mathbf{0.7264}$ (e) ROHIM $E_{linF,avg} = 0.8808$ (f) $Hint\text{-}F\mathfrak{C}_{fz}$ $E_{linF,avg} = 0.8100$

Fig. 9. Output images of raw image I24 of image database TID2013 produced by operators under consideration for human visual perception.

difficult than the indirect one, but it may offer a high potential to seek for a method of reaching an appropriate balance between global information and the local one of an image.

In this study, we follow the direct approach and propose a new formalism, in which the above S function can be constructed based on expert linguistic rules. This feature is very important as it permits, for first time, to utilise human expert domain knowledge to solve the ICE problem. Basically, when we could formally handle this linguistic knowledge, we would be able to simulate human capabilities in handling linguistic words to solve practical problems properly. This requires applying HAs, as mathematical models of word domains, to examine the problem. The main idea is as follows: because word domains in practice are finite, every linguistic rule-based knowledge formulated by a human expert to improve the image quality should represent a linguistic S function in the Cartesian product of finite word domains of the luminance variables of a raw image and of its output image. Thus, the key problem is how one can properly transform such a linguistic discrete S function into a numeric S function in $[L_{\min}, L_{\max}]^2$.

The study achieves the following new results:

• *Introduce a new HA formalism for developing image CIs*. The theory of HAs can provide a strict mathematical formalism to immediately handle the words of variables with their own inherent meaning. It forms a basis for developing methods enabling the developer to transform a linguistic S function mentioned above into a numeric S function in $[L_{\min}, L_{\max}]^2$, so that the semantics of LKBs are preserved. Although in Section 2.2 and Section 3.2, only minimally necessary notions and techniques of the HA formalism are provided, technically, they are sufficient for developing such methods. The way to construct *Hint* is an example for illustration.

• *Some main effective techniques to change the image contrast*. First is the homogeneity measurement HO_{MP} of each pixel window, which is carefully determined from examining more than 30 aggregation operators of the four components examined in [21] and HO_{MP} defined by (27) is the best. Experimentally, it is shown that it actually contributes to improve the image quality. Second is, for the first time, to apply a standard FCM to decompose an image into C fuzzy clusters based on the similarity of its pixel luminance values before the operator *Hint* is applied to its image channels. As each fuzzy cluster conveys certain global features of the given image revealed by a similarity measure calculated by the FCM, the value $F_{k,ij}(l)$ of the fuzzificator F_k of each entire channel i_k defined by (22) may convey the global image feature of each fuzzy cluster. Thus, *Hint* applied to $F_{k,ij}(l)$ instead of the luminance l itself can reach a reasonable balance in preserving the revealed global image feature as well as local details when changing the luminance.

• *Propose an image contrast intensification method Hint-F$\mathfrak{C}_{fz}$.* It is a novel method characterised by its specific way of changing the input image luminance that can be defined by (i) a human expert LKB for the whole input multichannel image; (ii) the pre-specified fuzziness parameter values of the linguistic luminance variables of the input and output image to determine their word semantics at each image pixel p_{ij}; and (iii) local image features at p_{ij} examined [21] to define the homogeneity HO_{MP} in formula (27). Its performance is validated by a comparative study with four selected counterpart methods, namely ESIHE (2014), RICE (2015), GHMF (2015), and ROHIM (2017). All methods are run on 27 images, including 24 of total 25 images of the image database TID2013 [63]. The obtained experiment results show that *Hint-F$\mathfrak{C}_{fz}$*, in general, outperforms the counterpart methods based on the objective criteria, i.e. $E_{avg}(\mathrm{i})$ and $E_{linF,avg}(\mathrm{i})$, and by human visual perception. Especially, the outputs of *Hint-F$\mathfrak{C}_{fz}$* are obviously more colourful and many of their features are more clearly visible. This means that *Hint-F$\mathfrak{C}_{fz}$* can reveal more details than the counterparts do.

Because the proposed method examined in this study is relatively new based on a strict mathematical formalism, to close the conclusions, we raise the following problems for further study:

- Problems related to expert capabilities in handling LKBs: The LKB consisting of only five rules and their words used in this study are still very simple. The question is whether image *CI*s based on more complex LKBs may still be more effective.
- Because several factors may influence the quality of a transformation of linguistic S functions described by a given LKB into respective numeric S functions, e.g. interpolation methods and fuzziness parameter values, the question is how can one evaluate the influence of these factors on the image *CI* performance?

Acknowledgements

This research is funded by Vietnam National Foundation for Science and Technology Development (NAFOSTED) under Grant No. 102.01-2017.06, and it is also supported in part by the Vietnam Academy of Science and Technology under the grant VAST01.05/15-16. We are also very grateful to Mr. K. Gu for his permission to use the programs of the methods ROHIM, RICE, and GHMF for our comparative studies.

Appendix A. Proof of Lemma 1

To show the validity of inequality (i), we consider the function $g(a) = (1-a)^{\tau}(1+\tau a) - (1+a)^{\tau}(1-\tau a)$, which is defined in [0, 1). As $\tau - 1 < 0$, it is easy to verify that

$$\frac{dg}{da} = (a+\tau a)\left[(1+a)^{\tau-1} - (1-a)^{\tau-1}\right] < 0,$$

which ensures that g is strictly increasing with respect to a in (0, 1). Thus, for all $a > 0$, $g(a) < g(0) = 0$, which leads to the inequality (i).

To prove (a) of (ii), we first keep in mind that the function $f^*(l) = \frac{1-l}{1+l} = \frac{2}{1+l} - 1$ is strictly decreasing in [0, 1]. Let us consider the function $f(t) = \left(\frac{1-l}{1+l}\right)^t$ also defined in [0, 1]. Clearly, for $\tau \in (0, 1)$, we have $f(0) = 1 > \frac{1-\tau l}{1+\tau l}$ and $f(1) = \frac{1-l}{1+l} < \frac{1-\tau l}{1+\tau l}$, where the last inequality follows from the monotonicity of f^* and from $l > \tau l$. Thus, there exists $t = \gamma$ that satisfies the equality in (a), with $l = a$. By (i) and the hypothesis of (ii), we have $\frac{1-\gamma a}{1+\gamma a} > \left(\frac{1-a}{1+a}\right)^{\gamma} = \frac{1-\tau a}{1+\tau a}$, which also from the strict monotonicity of f^* follows the inequality $\gamma < \tau$,. This shows the validity of the inequality in (a).

To prove (b) of (ii), we consider the function $f_1(l) = \ln\left(\frac{1+\tau l}{1-\tau l}\right)/\ln\left(\frac{1+l}{1-l}\right)$ defined in (0, 1). Because it can be verified that $d\left(\frac{1+\tau l}{1-\tau l}\right)/dl = \frac{2\tau}{(1-l)^2}$ and $d\left(\frac{1+l}{1-l}\right)/dl = \frac{2}{(1-l)^2}$, we have $\frac{df_1}{dl} = \frac{2}{[\ln((1+l)/(1-l))]^2(1-\tau^2l^2)(1-l^2)}\left\{\tau\left(1-l^2\right)\ln\left(\frac{1+l}{1-l}\right) - (1-\tau^2l^2)\ln\left(\frac{1+\tau l}{1-\tau l}\right)\right\} = 2/[\ln(1+l)(1-l)]^2(1-\tau^2l^2)(1-l^2) \times f_2(l)$, where $f_2(l) = \tau\left(1-l^2\right)\ln\left(\frac{1+l}{1-l}\right) - \left(1-\tau^2l^2\right)\ln\left(\frac{1+\tau l}{1-\tau l}\right)$ defined in [0, 1). Clearly, $f_2(0) = 0$ and we have $\frac{df_2}{dl} = 2\tau l\left\{-\ln\left(\frac{1+l}{1-l}\right) + \tau\ln\left(\frac{1+\tau l}{1-\tau l}\right)\right\}$. As $0 < \tau l < l < 1$ and f^* is strictly decreasing, we infer that $\ln\left(\frac{1+l}{1-l}\right) > \ln\left(\frac{1+\tau l}{1-\tau l}\right) > \tau\ln\left(\frac{1+\tau l}{1-\tau l}\right)$. This implies that $\frac{df_2}{dl} < 0$, and hence, $f_2(l)$ is also strictly decreasing. Thus, $f_2(l) < 0$, which results in the strictly decreasing monotonicity of f_1 on (0, 1).

Now, to compute $f_1(a)$, by statement (a) of (ii), we have $\left(\frac{1-a}{1+a}\right)^{\gamma} = \frac{1-\tau a}{1+\tau a}$, or equivalently, $\left(\frac{1+a}{1-a}\right)^{\gamma} = \frac{1+\tau a}{1-\tau a}$, which leads to $f_1(a) = \gamma$ by using the exponential function. As f_1 is strictly decreasing, for $\forall l \in (0, a)$, we have $f_1(l) = \ln\left(\frac{1+\tau l}{1-\tau l}\right)/\ln\left(\frac{1+l}{1-l}\right) > \gamma$. It implies that $\ln\left(\frac{1+\tau l}{1-\tau l}\right) > \gamma\ln\left(\frac{1+l}{1-l}\right)$, and hence, $\frac{1+\tau l}{1-\tau l} > \left(\frac{1+l}{1-l}\right)^{\gamma}$, or equivalently, $\frac{1-\tau l}{1+\tau l} < \left(\frac{1-l}{1+l}\right)^{\gamma}$, which is just the first desired inequality in (b).

By the same argument, the second inequality in (b) is also valid.

Appendix B. Proof of Theorem 1

(i) We prove first that *Hint* is a *CI*. By (26), for $l \in [0, \theta]$, we have $Hint_\theta(l) = \mathcal{C}_{\mathbb{c},\theta}^{-1} \circ CE \circ \mathcal{C}_{\mathbb{c},\theta}(l)$, and thus, $\mathcal{C}_{\mathbb{c},\theta}(Hint_\theta(l)) = CE(\mathcal{C}_{\mathbb{c},\theta}(l)) \geq \mathcal{C}_{\mathbb{c},\theta}(l)$, by the definition of *CE*. Because $\mathcal{C}_{\mathbb{c},\theta}$ is strictly decreasing, this inequality implies that $Hint_\theta(l) \leq l$, for $l \in [0, \theta]$. Similarly, for $l \in [\theta, 1]$, by the θ-symmetric rule R_θ, we obtain $Hint_\theta(l) = 1 - Hint_{\bar{\theta}}(1-l) \geq 1-(1-l) = l$. Consequently, $Hint_\theta$ is an operator *CI*.

To prove the equality in (i), by (28), we have $Hint_\theta(l) = \mathcal{C}_{\mathbb{c},\theta}^{-1}\left(\left(\frac{\theta-l}{\theta+l}\right)^{\gamma}\right) = l'$, for l in $[0, \theta]$, which implies that $\mathcal{C}_{\mathbb{c},\theta}\left(l'\right) = \frac{\theta-l'}{\theta+l'} = CE(\mathcal{C}_{\mathbb{c},\theta}(l))$. The last equality results in the first equality in (28) and the second one is immediately derived by rule R_θ.

(ii) It is obvious by its definition that $Hint_\theta(0) = 0$ and $Hint_\theta(\theta) = \theta$. For $l = \mathfrak{v}_{\mathcal{X}}\left(c^-\right) = \theta\beta_{\mathcal{X}}$, by (i), we have

$$\begin{aligned}
Hint_\theta\left(\mathfrak{v}_{\mathcal{X}}\left(c^-\right)\right) &= \theta\frac{1 - CE(\mathcal{C}_{\mathbb{c},\theta}(\theta\beta_{\mathcal{X}}))}{1 + CE(\mathcal{C}_{\mathbb{c},\theta}(\theta\beta_{\mathcal{X}}))} \\
&= \theta\left\{\left(1 - \left(\frac{\theta-\theta\beta_{\mathcal{X}}}{\theta+\theta\beta_{\mathcal{X}}}\right)^{\gamma}\right)\Big/\left(1 + \left(\frac{\theta-\theta\beta_{\mathcal{X}}}{\theta+\theta\beta_{\mathcal{X}}}\right)^{\gamma}\right)\right\} \\
&= \theta\left\{\left(1 - \left(\frac{1-\beta_{\mathcal{X}}}{1+\beta_{\mathcal{X}}}\right)^{\gamma}\right)\Big/\left(1 + \left(\frac{1-\beta_{\mathcal{X}}}{1+\beta_{\mathcal{X}}}\right)^{\gamma}\right)\right\} \\
&= \theta\left\{\left(1 - \left(\frac{1-m\beta_{\mathcal{X}}}{1+m\beta_{\mathcal{X}}}\right)\right)\Big/\left(1 + \left(\frac{1-m\beta_{\mathcal{X}}}{1+m\beta_{\mathcal{X}}}\right)\right)\right\} \\
&= \theta\left\{\left(1 - \left(\frac{1-m\beta_{\mathcal{X}}}{1+m\beta_{\mathcal{X}}}\right)\right)\Big/\left(1 + \left(\frac{1-m\beta_{\mathcal{X}}}{1+m\beta_{\mathcal{X}}}\right)\right)\right\} \\
&= \theta\beta_{\mathcal{Y}}^2 = \mathfrak{v}_{\mathcal{Y}}(very_c^-)
\end{aligned}$$

Applying the θ-symmetric rule R_θ to $Hint_\theta$, we obtain $Hint_\theta\left(\mathfrak{v}_{\mathcal{X}}\left(c^+\right)\right) = \mathfrak{v}_{\mathcal{Y}}\left(very\_c^+\right)$ and $Hint_\theta(1) = 1$. Therefore, we have proved that *Hint* runs through the five points in (21).

To prove the equalities of (ii), for $\gamma = \gamma(\beta_{\mathcal{X}}, m)$, it follows from (b) of (ii) in Lemma 1 that $\frac{1-ml}{1+ml} < \left(\frac{1-l}{1+l}\right)^{\gamma}$, where $l \in [0, \beta_{\mathcal{X}}]$. For $l \in [0, \mathfrak{v}_{\mathcal{X}}\left(c^-\right)) = [0, \theta\beta_{\mathcal{X}})$, putting $l' = \frac{l}{\theta} \in [0, \beta_{\mathcal{X}}]$, we have $\frac{1-l'}{1+l'} = \frac{\theta-l}{\theta+l}$, and by (a) and (b) in (ii) of Lemma 1, we also have $\left(\frac{1-\beta_{\mathcal{X}}}{1+\beta_{\mathcal{X}}}\right)^{\gamma} = \left(\frac{1-m\beta_{\mathcal{X}}}{1+m\beta_{\mathcal{X}}}\right)$ and $\frac{1-ml}{1+ml} < \left(\frac{1-l}{1+l}\right)^{\gamma}$, which is equivalent to the inequality $\frac{\theta-ml}{\theta+ml} < \left(\frac{\theta-l}{\theta+l}\right)^{\gamma}$. By the definition of $\mathcal{C}_{\mathbb{c},\theta}$ and *CE*, it follows from (27) that $\mathcal{C}_{\mathbb{c},\theta}(ml) < CE(\mathcal{C}_{\mathbb{c},\theta}(l)) = \mathcal{C}_{\mathbb{c},\theta}(Hint_\theta(l))$. Because $\mathcal{C}_{\mathbb{c},\theta}$ is strictly decreasing in $[0, \theta]$, we infer that $Hint_\theta(l) < ml$. Recall that $Hint_\theta(\theta\beta_{\mathcal{X}}) = Hint_\theta\left(\mathfrak{v}_{\mathcal{X}}\left(c^-\right)\right) = \mathfrak{v}_{\mathcal{Y}}\left(very\_c^-\right) = \theta\beta_{\mathcal{Y}}^2$; thus, the last inequality results in $\frac{Hint_\theta(l)}{l} < m = \frac{\beta_{\mathcal{Y}}^2}{\beta_{\mathcal{X}}} = \frac{Hint_\theta\left(\mathfrak{v}_{\mathcal{X}}\left(c^-\right)\right)}{\mathfrak{v}_{\mathcal{X}}\left(c^-\right)}$, for all $l \in (0, \mathfrak{v}_{\mathcal{X}}\left(c^-\right)]$. Because $\frac{Hint_\theta(l)}{l}$ is continuous in $[0, \theta]$, it follows that $\max_{l\in(0,\mathfrak{v}_{\mathcal{X}}(c^-))}\frac{Hint_\theta(l)}{l} = m$.

From (b) of (ii) in Lemma 1, for $\gamma = \gamma(\beta_{\mathfrak{X}}, m)$, we infer that $\left(\frac{1-l'}{1+l'}\right)^{\gamma} < \frac{1-ml'}{1+ml'}$, where $l' = \frac{l}{\theta} \in [\beta_{\mathfrak{X}}, 1]$. By a similar argument as above, for the case $l' = \frac{l}{\theta} \in [0, \beta_{\mathfrak{X}}]$, we have $\frac{Hint_{\theta}(l)}{l} > m = \frac{\beta^2_{\mathfrak{Y}}}{\beta_{\mathfrak{X}}} = \frac{Hint_{\theta}\left(\mathfrak{v}_{\mathfrak{X}}(c^-)\right)}{\mathfrak{v}_{\mathfrak{X}}(c^-)}$, for all $l \in [\theta\beta_{\mathfrak{X}}, \theta] = [\mathfrak{v}_{\mathfrak{X}}\left(c^-\right), \theta]$, and hence, $\min_{l\in(\mathfrak{v}_{\mathfrak{X}}(c^-),\theta)} \frac{Hint_{\theta}(l)}{l} = m$.

As $\mathfrak{v}_{\mathfrak{X}}$ and $Hint_{\theta}$ are θ-symmetric functions, we can apply the θ-symmetric rule R_{θ} to $\min_{l\in(\mathfrak{v}_{\mathfrak{X}}(c^+),1)} \frac{1-Hint_{\bar{\theta}}(1-l)}{1-l}$, in which $Hint_{\theta}(l)$, l, and the interval $(\mathfrak{v}_{\mathfrak{X}}\left(c^+\right), 1)$ are transformed respectively into $1 - Hint_{\bar{\theta}}(1-l)$, $(1-l)$, and $(0, \mathfrak{v}_{\mathfrak{X}}\left(c^-\right))$. Then, we obtain

$$\begin{aligned}
&\min_{l\in(\mathfrak{v}_{\mathfrak{X}}(c^+),1)} \frac{1 - Hint_{\bar{\theta}}(1-l)}{1-l} \\
&= \max_{l\in(0,\mathfrak{v}_{\mathfrak{X}}(c^-))} \frac{1 - (1 - Hint_{\theta}\,(1-(1-l)))}{1-(1-l)} \\
&= \max_{l\in(0,\mathfrak{v}_{\mathfrak{X}}(c^-))} \frac{Hint_{\theta}\,(l)}{l} = m
\end{aligned}$$

which is the desired equality. Because the proof of the remaining equality is similar, the equalities in (ii) are completely proved. □

Appendix C. Proof of Theorem 2

(i) By the hypothesis of the theorem, $m = \xi$, and (a) of (ii) of Lemma 1, we have $\gamma = \gamma(\beta, \xi) < m = \xi$, where $\gamma \in (0, 1)$. Thus, for $\forall t$, $\gamma \in (0, 1)$, the validity of the inequality in (i) is easily deduced from the fact that $\gamma < \xi^t$. For $t = 0$, the inequality is deduced immediately from $\gamma < 1$ and $\mathcal{C}_{\mathbb{c},\theta}\,(l) < 1$. For $t = 1$, also by (a) of (ii) in Lemma 1, we clearly infer that, for any $\xi \in (0, 1]$, $\gamma = \ln\left(\frac{1+\xi\beta}{1-\xi\beta}\right)/\ln\left(\frac{1+\beta}{1-\beta}\right) = \ln\left(\frac{2}{1-\xi\beta} - 1\right)/\ln\left(\frac{1+\beta}{1-\beta}\right)$, which is increasing in ξ, and that $\gamma < \xi$. Obviously, $CE = \left(\mathcal{C}_{\mathbb{c},\theta}(l)\right)^{\xi}$ is decreasing in ξ, and hence, the inequality in (ii) holds.

(ii) Assume that $l \in [0, \beta \mathrm{fm}(c^-)] = [0, \beta\theta]$, which is the fuzziness interval of $c^- = low$, and put $z = \frac{l}{\theta} \in [0, \beta]$. By Cheng's method, for $t \in [0, 1]$, we have

$$\begin{aligned}
CI_{Ch}(l) &= \mathcal{C}^{-1}_{\mathbb{c},\theta}(CE_{Ch}(\mathcal{C}_{\mathbb{c},\theta}(l))) = C^{-1}_{\mathbb{c},\theta}\left(\left(C_{\mathbb{c},\theta}(l)\right)^{\xi^t}\right) \\
&= \theta\frac{1-\left(\frac{\theta-l}{\theta+l}\right)^{\xi^t}}{1+\left(\frac{\theta-l}{\theta+l}\right)^{\xi^t}} = \theta\frac{1-\left(\frac{1-z}{1+z}\right)^{\xi^t}}{1+\left(\frac{1-z}{1+z}\right)^{\xi^t}}
\end{aligned}$$

Because it is observed that the function $f\,(z) = \frac{1-z}{1+z} = \frac{2}{1+z} - 1$ is decreasing in $(0, 1)$ and by (i) of Lemma 1 $\left(\frac{1-z}{1+z}\right)^{\xi^t} < \frac{1-\xi^t z}{1+\xi^t z}$, we have $\theta\frac{1-\left(\frac{1-z}{1+z}\right)^{\xi^t}}{1+\left(\frac{1-z}{1+z}\right)^{\xi^t}} \geq \theta\frac{1-\frac{1-\xi^t z}{1+\xi^t z}}{1+\frac{1-\xi^t z}{1+\xi^t z}} = \theta\xi^t z = \xi^t l > \xi l = ml$. For $l \in [0, \beta\theta] = [0, \mathfrak{v}_{\mathfrak{X}}\left(c^-\right)]$, by (ii) of Theorem 1, it follows that $Hint_{\theta}(l) < CI_{Ch}(l)$.

References

[1] D. Chang, W. Wu, Image contrast enhancement based on a histogram transformation of local standard deviation, IEEE Trans. Med. Imaging 17 (4) (1998) 518–531.
[2] M. Abdullah-Al-Wadud, Md. Hasanul Kabir, M. Ali Akber Dewan, Oksam Chae, A dynamic histogram equalization for image contrast enhancement, IEEE Trans. Consum. Electron. 53 (2) (2007) 593–600.
[3] T.K. Agarwal, M. Tiwari, S.S. Lamba, Modified histogram based contrast enhancement using homomorphic filtering for medical images, in: IEEE Int. Advance Comput. Conf., 2014, pp. 964–968.
[4] T.-L. Ji, Tucson, M.K. Sundareshan, H. Roehrig, Adaptive image contrast enhancement based on human visual properties, IEEE Trans. Med. Imaging 13 (4) (2002) 573–586.
[5] A. Ziaei, H. Yeganeh, K. Faez, S. Sargolzaei, A novel approach for contrast enhancement in biomedical images based on histogram equalization, in: Int. Conf. on BioMedical Engineering and Informatics, no. 1, 2008, pp. 855–858.
[6] Y. Kimori, Morphological image processing for quantitative shape analysis of biomedical structures: effective contrast enhancement, J. Synchrotron Radiat. (2013) 848–853.
[7] Kirti Khatkar, Dinesh Kumar, Biomedical image enhancement using wavelets, Procedia Comput. Sci. Volume 48 (2015) 513–517.
[8] D.J. Jobson, Z. Rahman, G.A. Woodell, G.D. Hines, A comparison of visual statistics for the image enhancement of foresite aerial images with those of major image classes, in: Visual Information Processing XV, 2006.
[9] B. Attachoo, Pattanasethanon, A new approach for colored satellite image enhancement, in: Robotics and Biomimetics, IEEE Int. Conf., 2008, pp. 1365–1370.
[10] Hasan Demirel, Cagri Ozcinar, Gholamreza Anbarjafari, Satellite image contrast enhancement using discrete wavelet transform and singular value decomposition, IEEE Geosci. Remote Sensing Lett. 7 (2) (2010) 333–337.
[11] H. Tasmaz, H. Demirel, G. Anbarjafari, Satellite image enhancement by using dual tree complex wavelet transform: Denoising and illumination enhancement, in: Signal Processing and Communications Applications Conference, SIU, 2012, 2012, April, pp. 1–4.
[12] D.-Ch. Tseng, Ch.-L. Chien, A cloud removal approach for aerial image visualization, Int. J. Innov. Comput. Inf. Control 9 (6) (2013) 2421–2440.
[13] Salem Saleh Al-amri, N.V. Kalyankar, S.D. Khamitkar, Linear and non-linear contrast enhancement image, Int. J. Comput. Sci. Netw. Secur. 10 (2) (2010) 139–143.
[14] Xu. Xiaoyin, E.L. Miller, Entropy optimized contrast stretch to enhance remote sensing imagery, in: 16th Int. Conf. on Pattern Recognition, ICPR'02, no. 3, 2002.
[15] S. Kalchmair, N. Jährling, K. Becker, H.-U. Dodt, Image contrast enhancement in confocal ultramicroscopy, Opt. Lett. 35 (1) (2010) 79–81.
[16] N.S.P. Kong, H. Ibrahim, Ch.H. Ooi, D.Ch.J. Chieh, Enhancement of microscopic images using modified self-adaptive plateau histogram equalization, in: Computer Technology and Development, Int. Conf. vol. 2, 2009, pp. 308–310.
[17] Biswajit Biswas, Pritha Roy, Ritamshirsa Choudhuri, Biplab Kanti Sen, Microscopic image contrast and brightness enhancement using multi-scale retinex and cuckoo search algorithm, Procedia Comput. Sci. 70 (2015) 348–354.
[18] J. Tang, X. Liu, Q. Sun, A direct image contrast enhancement algorithm in the wavelet domain for screening mammograms, IEEE J. Sel. Top. Sign. Proces. 3 (1) (2009) 74–80.
[19] Mohd Helmy Abd Wahab, Nasriah Zakaria, Rohaya Latip, Rosalina Abdul Salam, Image contrast enhancement for outdoor machine vision applications, in: Int. Conf. of Soft Computing and Pattern Recognition, SoCPaR, 2013, pp. 377–383.
[20] T. Chaira, An improved medical image enhancement scheme using Type II fuzzy set, Appl. Soft Comput. 25 (2014) 293–308.
[21] H.D. Cheng, Mei Xue, X.J. Shi, Contrast enhancement based on a novel homogeneity measurement, Pattern Recognit. 36 (2003) 2687–2697.
[22] H.D. Cheng, H.J. Xu, A novel fuzzy logic approach to contrast enhancement, Pattern Recognit. 33 (2000) 809–819.
[23] F. Farbiz, M.B. Menhaj, S.A. Motamedi, M.T. Hagan, A new fuzzy logic filter for image enhancement, IEEE Trans. Syst. Man Cybernet. 30 (1) (2000) 110–119.
[24] M. Hanmandlu, M. Jha, R. Sharma, Color image enhancement by fuzzy intensification, Pattern Recognit. Lett. 24 (1–3) (2003) 81–87.
[25] M. Hanmandlu, O.P. Verma, N.K. Kumar, M. Kulkarni, A novel optimal fuzzy system for color image enhancement using bacterial foraging, IEEE Trans. Instrum. Meas. 58 (8) (2009) 2867–2879.
[26] S. Hashemi, S. Kiani, N. Noroozi, M.E. Moghaddam, An image contrast enhancement method based on genetic algorithm, Pattern Recognit. Lett. 31 (13) (2010) 1816–1824.
[27] Kh. Hasikin, N.A. Mat Isa, Enhancement of the low contrast image using fuzzy set theory, in: Int. Conf. on, Computer Modeling and Simulation, 2012, pp. 371–376.
[28] Balasubramaniam Jayaram, Kakarla V.V.D.L Narayana, V. Vetrivel, fuzzy inference system based contrast enhancement, EUSFLAT-LFA, 2011.
[29] B. Jayaram, Kakarla V.V.D.L. Narayana, V. Vetrivel, Fuzzy inference system based contrast enhancement, in: Eusflat'2011, Aix-les-Bains, France, 2011, pp. 311–318.
[30] H. Kundra, Er. Aashima, Er.M. Verma, Image enhancement based on fuzzy logic, IJCSNS Int. J. Comput. Sci. Netw. Secur. 9 (10) (2009) 141–145.
[31] H. Li, H.S. Yang, Fast and reliable image enhancement using fuzzy relaxation technique, IEEE Trans. Syst. Man. Cybern. 19 (5) (1989) 1276–1281.
[32] S.K. Pal, R.A. King, Image enhancement using fuzzy sets, IEEE Electron. Lett. 16 (10) (1980) 376–378.
[33] S.K. Pal, R.A. King, Image enhancement using smoothing with fuzzy sets, IEEE Trans. Syst. Man Cybern. 11 (7) (1981) 494–501.
[34] M. Russo, G. Ramponi, A fuzzy operator for the enhancement of blurred and noisy images, IEEE Trans. Image Process. 4 (8) (1995) 1169–1174.
[35] G. Sudhavani, M. Srilakshmi, P.Venkateswara Rao, Comparison of fuzzy contrast enhancement techniques, Int. J. Comput. Appl. 95 (22) (2014) 26–31.
[36] V. Kim, L. Taroslavaski, Rank algorithms for picture processing, Comput. Vis. Graph. Image Process. 35 (1986) 234–258.

[37] R. Gordon, R.M. Rangayan, Feature enhancement of film mammographic features using fixed and adaptive neighborhoods, Appl. Opt. 23 (13) (1984) 560–564.
[38] A.P. Dhnawan, G. Buelloni, R. Gordon, Enhancement of mammographic features by opti-mal adaptive neighborhood image processing, IEEE Trans. Med. Imaging 5 (1986) 8–15.
[39] R.C. Gonzalez, R.E. Woods, Digital Image Processing, Prentice Hall, New Jersey, 2008.
[40] S.S. Agaian, S. Blair, K.A. Panetta, Transform coefficient histogram-based image enhancement algorithms using contrast entropy, IEEE Trans. Image Process. 16 (3) (2007) 741–758.
[41] A.O. Boudraa, E.H.S. Diop, Image contrast enhancement based on 2D teager-kaiser operator, in: Proc. of the IEEE Int. Conf. on Image Process, 2008, pp. 3180–3183.
[42] J. Soha, A.A. Schwartz, in: Proc. 5th Canad. Symp. Remote Sensing, 1978, pp. 86–93 Multi-dimensional histogram normalization contrast enhancement,
[43] S. Lee, An efficient content-based image enhancement in the compressed domain using retinex theory, IEEE Trans. Circuits Syst. Video Technol. 17 (2) (2007) 199–213.
[44] A. Beghdadi, A.L. Negrate, Contrast enhancement technique based on local detection of edges, Comput. Vis. Graph. Image Process. 46 (1989) 162–174.
[45] L. Dash, B.N. Chatterji, Adaptive contrast enhancement and de-enhancement, Pattern Recognit. 24 (1991) 289–302.
[46] M. Hanmandlu, D. Jha, An optimal fuzzy system for color image enhancement, IEEE Trans. Image Process. 15 (10) (2006) 2956–2966.
[47] C.H. Nguyen, W. Wechler, Hedge algebras: An algebraic approach to structures of sets of linguistic domains of linguistic truth variable, Fuzzy Sets and Systems 35 (3) (1990) 281–293.
[48] C.H. Nguyen, W. Wechler, Extended hedge algebras and their application to fuzzy logic, Fuzzy Sets and Systems 52 (1992) 259–281.
[49] C.H. Nguyen, W. Pedrycz, Th.L. Duong, Th.S. Tran, A genetic design of linguistic terms for fuzzy rule based classifiers, Int. J. Approx. Reason. 54 (2013) 1–21.
[50] C.H. Nguyen, Th.S. Tran, D.Ph. Pham, Modeling of a semantics core of linguistic terms based on an extension of hedge algebra semantics and its application, Knowl. Based Syst. 67 (2014) 244–262.
[51] C.H. Nguyen, V.N. Huynh, W. Pedrycz, A construction of sound semantic linguistic scales using 4-tuple representation of term semantics, Internat. J. Approx. Reason. 55 (2014) 763–786.
[52] C.H. Nguyen, V. Th. Hoang, V.L. Nguyen, A discussion on interpretability of linguistic rule based systems and its application to solve regression problems, Knowl. Based Syst. 88 (2015) 107–133.
[53] C.H. Nguyen, Nh.L. Vu, X.V. Le, Quantifying hedge algebras interpolative reasoning method and its application to some problems of fuzzy control, WSEAS Trans. Comput. 11 (5) (2006) 2519–2529.
[54] C.H. Nguyen, N.L. Vu, X.V. Le, Optimal hedge-algebras-based controller: Design and Application, Fuzzy Sets and Systems 159 (2008) 968–989.
[55] H.L. Bui, D.Tr. Tran, Nh.L. Vu, Optimal fuzzy control of inverted pendulum, J. Vib. Control 18 (14) (2012) 2097–2110.
[56] H.L. Bui, D.D. Nguyen, Nh.L Vu, D.Tr. Tran, A study on the application of hedge algebras to active fuzzy control of a seism-excited structure, J. Vib. Control 18 (14) (2012) 2186–2200.
[57] H.L. Bui, D.A. Nguyen, D.Tr. Tran, Nh.L. Vu, Application of hedge algebra-based fuzzy controller to active control of a structure against earthquake, Struct. Control Health monit. 20 (2013) 483–495.
[58] H.L. Bui, C.H. Nguyen, N.L. Vu, C.H. Nguyen, General design method of hedge-algebras-based fuzzy controllers and an application for structural active control, Appl. Intell. 43 (2015) 251–275.
[59] D. Vukadinović, M. Bašić, C.H. Nguyen, N.L. Vu, T.D. Nguyen, Hedge-Algebra-Based voltage controller for a self-excited induction generator, Control Eng. Pract. 30 (2014) 78–90.
[60] C.H. Nguyen, V.N. Huynh, An algebraic approach to linguistic hedges in zadeh fuzzy logic, Fuzzy Sets and Systems 129 (2002) 229–254.
[61] C.H. Nguyen, A topological completion of refined hedge algebras and a model of fuzziness of linguistic terms and hedges, Fuzzy Sets and Systems 158 (4) (2007) 436–451.
[62] C.H. Nguyen, V.L. Nguyen, Fuzziness measure on complete hedge algebras and quantifying semantics of terms in linear hedge algebras, Fuzzy Sets and Systems 158 (4) (2007) 452–471.
[63] N. Ponomarenko, L. Jin, O. Ieremeiev, V. Lukin, K. Egiazarian, J. Astola, B. Vozel, K. Chehdi, M. Carli, F. Battisti, C.-C. Jay Kuo, Image database TID2013: Peculiarities, results and perspectives, Signal Process., Image Commun. 30 (2015) (2013) 57–77.
[64] K. Singh, R. Kapoor, Image enhancement using exposure based sub image histogram equalization, Pattern Recognit. Lett. 36 (2014) 10–14.
[65] K. Gu, G. Zhai, X. Yang, W. Zhang, Ch.W. Chen, Automatic contrast enhancement technology with saliency preservation, IEEE Trans. Circuits Syst. Video Technol. (T-CSVT) 25 (9) (2015) 1480–1494.
[66] K. Gu, G. Zhai, Sh. Wang, M. Liu, J. Zhou, W. Lin, A general histogram modification framework for efficient contrast enhancement, in: Proc. IEEE Int. Symp. Circuits and Syst., ISCAS, May 2015, pp. 2816–2819.
[67] K. Gu, W. Lin, G. Zhai, X. Yang, W. Zhang, C.W. Chen, No-reference quality metric of contrast-distorted images based on information maximization, IEEE Trans. Cybern. 47 (12) (2017) 4559–4565.
[68] M.M. Gupta, J. Qi, T heory of T-norms and fuzzy inference methods, Fuzzy Sets and Systems 40 (1991) 431–450.
[69] https://sites.google.com/site/guke198701/publications.
[70] Output images of the 24 raw images in TID2013, http://ees.elsevier.com/asoc/download.aspx?id=620074&guid=eea66406-8fe6-48a5-86d7-7fa3a7790674&scheme=1.